Pennsylvanian Fusulinids From Southeastern Alaska

By RAYMOND C. DOUGLASS

GEOLOGICAL SURVEY PROFESSIONAL PAPER 706

A fauna of Middle Pennsylvanian age showing similarities with faunas from Japan and central British Columbia, Canada

UNITED STATES GOVERNMENT PRINTING OFFICE, WASHINGTON : 1971

UNITED STATES DEPARTMENT OF THE INTERIOR

ROGERS C. B. MORTON, *Secretary*

GEOLOGICAL SURVEY

William T. Pecora, *Director*

Library of Congress catalog—card No. 77–611482

For sale by the Superintendent of Documents, U.S. Government Printing Office
Washington, D.C. 20402 - Price 70 cents (paper cover)

CONTENTS

ILLUSTRATIONS

[Plates follow index]

TABLES

PENNSYLVANIAN FUSULINIDS FROM SOUTHEASTERN ALASKA

By Raymond C. Douglass

ABSTRACT

A fusulinid fauna from the Klawak Formation and Ladrones Limestone of Prince of Wales Island in southeastern Alaska includes eight genera of fusulinids and some smaller Foraminifera. The fauna is similar to faunas of Middle Pennsylvanian age described from north-central British Columbia in Canada, and from parts of central Japan. Four of the taxa are new including *Pseudostaffella rotunda* n. sp., *Fusulinella pinguis* n. sp., *Fusulinella alaskensis* n. sp., and *Fusulina flexuosa* n. sp.

INTRODUCTION

PREVIOUS WORK

The scarcity of evidence of marine rocks of Pennsylvanian age in Alaska was summarized by Dutro and Douglass (1961, p. B239). Rocks of Middle Pennsylvanian age were identified in Saginaw Bay at the north end of Kuiu Island. At that locality fusulinids were recognized along with a varied megafauna. Muffler (1967, p. C19) assigned these rocks to the Saginaw Bay Formation of Carboniferous age.

CURRENT STUDY

In 1966 A. K. Armstrong collected a series of samples from measured sections of the Klawak Formation in the areas north of Craig and the Ladrones Limestone south of Craig, Prince of Wales Island. Samples were collected from every 10 feet or less through each section.

SIGNIFICANCE OF THE FUSULINID ASSEMBLAGES

The fusulinids represented in these samples include several genera characteristic of rocks of Middle Pennsylvanian age and include *Nankinella*, *Staffella*, *Pseudostaffella*, *Fusulinella*, and *Fusulina*. The species are relatively primitive forms and as such do not suggest latest Middle Pennsylvanian age. As no fusulinids have been identified in this general area below or above the samples studied, no definite limits can be determined for the age of the Klawak Formation and the Ladrones Limestone.

CORRELATION

The faunas described herein can be compared with faunas described from the Fort St. James area in central British Columbia, Canada, and with faunas described from as far away as Texas in the U.S.A. and from central Japan. The faunas described from central British Columbia by Thompson, Pitrat, and Sanderson (1953, p. 545) and by Thompson (1965, p. 224) include species assigned to each of the genera listed above and show similarity in stage of development. As I noted in the section on systematics, precise comparisons are difficult because of the paucity of data available for the Canadian material.

Comparison with the Texas faunas are even more difficult, but there is general similarity in the species of *Nankinella*, *Staffella*, *Pseudostaffella*, and *Fusulinella*. The counterpart of the *Fusulina* from Alaska and British Columbia has not been reported so far from the conterminous United States.

Faunas from three areas in Japan show similarities to the Alaskan fauna. The fauna described by Igo (1957, p. 167) from Fukuji in the Hida Massif of central Honshu contains species of *Nankinella*, *Staffella*, *Pseudostaffella*, and *Fusulinella* resembling those from Alaska. The Shishidedai area on the northern edge of the Akiyoshi Plateau in southern Honshu contains a fauna described by Toriyama (1953, p. 251, 1958, p. 5) with forms similar to the *Nankinella*, *Fusulinella*, and *Fusulina* from Alaska. The faunas of the-Itadorigawa Group of western Shikoku described by Ishii (1958a, b; 1962) also show similarities to those from Alaska.

Comparisons were also attempted with material from other parts of the world where generally similar forms have been described or illustrated. Among these, some similarities were recognized in material from Spitsbergen (Forbes 1960, p. 212) and from Spain (van Ginkel 1965, p. 159).

Wherever the fusulinid faunas of Middle Pennsylvanian age have been studied in detail, similarities at the generic level are obvious and the general character of the species is similar. Unfortunately, the data presented with most of the faunas previously described are inadequate for comparisons at the species level. Notable exceptions are the more fully documented studies by Ishii and van Ginkel.

LOCALITIES

The samples are from two areas in the vicinity of Craig, Prince of Wales Island (fig. 1*A*, *B*). The southernmost samples are from the Ladrones Islands, about 7 miles south-southeast of Craig (fig. 1*C*), and the northernmost samples are from the area north of Klawak and about 8 miles north-northeast of Craig (fig. 1*D*).

Locality 29.—Ladrones Islands, field section 66x16 of A. K. Armstrong, Ladrones Limestone.

f23973. Sample taken 10 ft above the base of the exposed section above high tide. Light-gray calcarenite largely composed of fossil fragments in a sparry calcite matrix. Fragments of echinoderms, gastropods, and fusulinids are common. *Tetrataxis* sp., endothyrids, *Nankinella* sp., and *Fusulinella pinguis* n. sp.

f23974. Sample taken 20 ft above the base of the exposed section above high tide. The lithology and fauna of this sample is similar to that of f23973.

Locality 30.—Peratovich Island, field section 66x4B of A. K. Armstrong, Klawak Formation.

f23975. Sample taken from 101 ft above the base of the section measured on the small peninsula trending north-northwest in the center of the north half sec. 35, T. 72 S., R. 80 E., Craig (C–4) quadrangle map. Dark-gray coarse calcarenite largely composed of fossil fragments in a silty lime mud matrix. Fragments of echinoderms, brachiopods, bryozoans, gastropods, and fusulinids are common. Textularids, *Millerella* sp., *Nankinella* sp., *Staffella* sp., and *Pseudostaffella rotunda* n. sp.

f23976. Sample taken from 106 ft above the base of the section at the same locality. The lithology and fauna of this sample are similar to that of f23975.

Locality 31.—Small unnamed island exposed at low tide between Peratovich Island and the main part of Prince of Wales Island and about 1.5 miles north of Klawak. Filled section 66x4C of A. K. Armstrong, Klawak Formation.

f23977. Sample from 20 ft above the base of the section. Medium-gray coarse calcarenite composed largely of fragments of fossils in a silty lime mud and sparry climate matrix Textularids, *Tetrataxis* sp., *Fusulinella alaskensis* n. sp., and *Fusulina flexuosa* n. sp.

f23978. Sample from 35 ft above the base of the section. Dark-greenish-gray calcareous siltstone with abundant fossil fragments including echinoderms, bryozoans, coral, brachiopods, gastropods, and fusulinids. Textularids, *Tetrataxis* sp., *Ozawainella*? sp., *Fusulinella* sp., and *Fusulina* sp.

f23979. Sample from 45 ft above the base of the section. Medium-gray coarse calcarenite with a silty to sparry calcite matrix. Fragments of echinoderms, bryozoans, brachipods, and Foraminifera. Textularids, *Textrataxis* sp., endothyrids including *Bradyina* sp., *Fusulinella alaskensis* n. sp., and *Fusulina flexuosa* n. sp.

f23980. Sample from 65 ft above the base at the section. Mostly a dark-greenish-gray calcareous siltstone grading into some calcarenite with fragments of fossils in a sparry calcite matrix. Echinoderms, bryozoans, and Foraminifera. Textularids, *Bradyina* sp., *Fusulinella alaskensis* n. sp., and *Fusulina flexuosa* n. sp.

f23981. Sample from 75 ft above the base of the section. Dark-gray coarse conglomeratic calcarenite with fragments of echinoderms, bryozoans, and fusulinids. *Fusulinella alaskensis* n. sp. and *Fusulina flexuosa* n. sp.

f23982. Sample from 80 ft above the base of the section. Medium-gray coarse calcarenite with fragments of echinoderms, bryozoans, and Foraminifera in a sparry calcite matrix. Textularids, *Tetrataxis* sp., *Bradyina* sp., and *Fusulinella alaskensis* n. sp.

Locality 32.—Ledges exposed at low tide on west shore of Prince of Wales Island about 1.5 miles north-northeast of Klawak. Field section 66x4D of A. K. Armstrong. Klawak Formation.

f23983. Sample from 20 ft above the base of the section. Light-gray medium-grained calcarenite with shell fragments in a sparry calcite matrix. *Tetrataxis* sp., *Bradyina* sp., and *Fusulinella* sp.

f23984. Sample from 40 ft above the base of the section. Light-gray fine- to medium-grained calcarenite with shell fragments in a sparry calcite matrix. Endothyrids including *Bradyina* sp. are present with a small *Fusulinella* sp.

f23985. Sample from 55 ft above the base of the section. Medium-yellowish-gray fine calcarenite with shell fragments in a sparry calcite matrix. Endothyrids and a small *Fusulinella* sp.

f23986. Sample from 60 ft above the base of the section. Medium-gray coarse conglomeratic calcarenite with subrounded clasts up to an inch across of other limestone and volcanic rocks. The matrix is a calcarenite with abundant shell fragments and fusulinids. Textularids, *Tetrataxis* sp., *Bradyina* sp., *Fusulinella alaskansis* n. sp., *Fusulina flexuosa* n. sp., and *Beedeina*?

DISPOSITION OF MATERIAL

The specimens used in this study are deposited in the collections of the U.S. National Museum (USNM), and specimen numbers are indicated on the plate explanations. The bulk material is filed in the U.S. Geological Survey collections at the U.S. National Museum under the sample numbers listed for each locality described in the preceding section of this report.

ACKNOWLEDGMENTS

I thank A. K. Armstrong for his careful collection of samples in measured sections from which those samples studied were selected. Richard Margerum did an outstanding job in the unusually difficult preparation of oriented thin sections of small fusulinids in a dark matrix. The computer programming and processing of numerical data were done by Nancy Cotner, Ralph Eicher, and Paul Zabel.

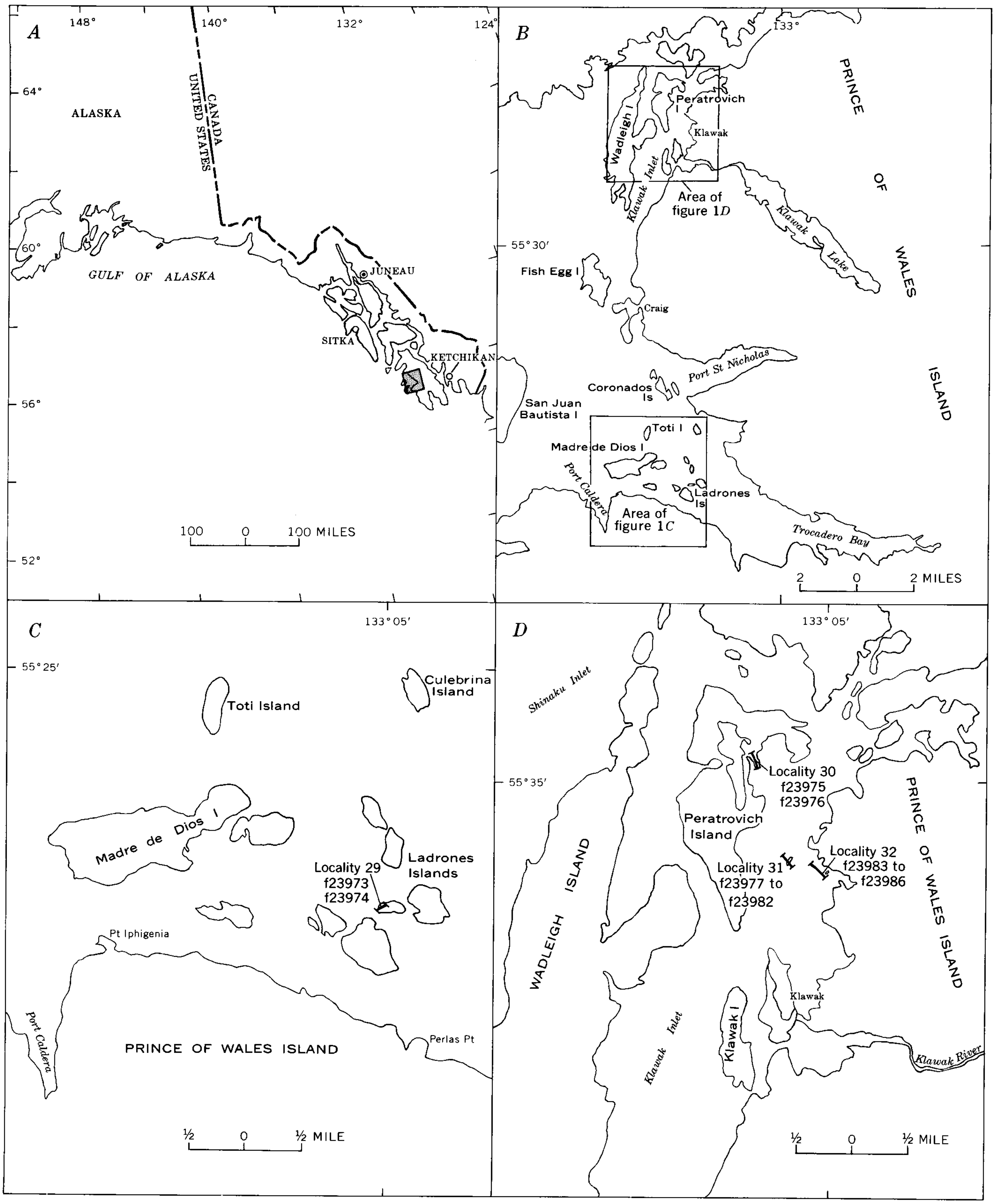

FIGURE 1.—Index maps. *A*. Southeastern Alaska and adjacent Canada showing area of this report (patterned). *B*. Part of Prince of Wales Island showing the Ladrones Islands and the Klawak area. *C*. The Ladrones Islands area showing locality 29. *D*. The Klawak area showing localities 30, 31, and 32.

METHODS OF STUDY

Each sample was sliced and etched lightly with dilute hydrochloric acid and coated with thinned clear lacquer. Samples that contained fusulinids were prepared for further study by making oriented thin sections of the fusulinids. Measurements of radius, volution height, half length, wall thickness, and tunnel width were made at each half volution on axial sections. Measurements of radius, volution height, wall thickness, and septal spacing were made at each half volution on equatorial sections. The maximum outer diameter of the proloculus was measured for each specimen.

The data obtained from these measurements, made at half volutions, was converted to equivalent values at standard radii by linear interpolation of values using a computer to determine the values at each standard radius. Thus the wall thickness for each specimen could be interpolated for a radius of 0.5 mm (millimeter) for instance, even though the actual measurement was a 0.43 mm or 0.52 mm. The interpolated values of each attribute at each standard radius were summarized for each species in every sample.

The standard radii were selected so that the logarithms to base 10 of adjacent radii are 0.1 apart. This gives about two points in each volution. The radii used (in millimeters) are 0.10, 0.13, 0.16, 0.20, 0.25, 0.32, 0.40, 0.50, 0.63, 0.79, 1.00, 1.26, and so on.

The statistical summaries provide values commonly needed for making comparisons between samples. How these values are derived is now common knowledge, and formulae used are given in Simpson, Roe, and Lewontin (1960). The computed values include the mean, variance, standard deviation, coefficient of variability, standard error of the mean, 95 percent confidence limits on the mean, and listing the observed maximum and minimum values for each attribute.

Graphs similar to those of Douglass (1970, p. G8–G9) showing the mean, confidence limits on the mean, and total observed variation for each attribute plotted against the standard radii were prepared from these data. The form ratio (half length/radius vector) was also computed at each radius and plotted in a similar manner.

When more than one sample contained the same species, the data were combined for the samples and all statistical values recalculated and replotted. Two samples were assumed to contain the same species if specimens were of the same genus and all their measurable attributes when compared at standard radii were similar.

Comparisons with previously named or described species were more difficult. In some instances (Ishii 1958a,b, 1962; van Ginkel, 1965) enough data were provided to compare the specimens at standard radii. In most instances data were insufficient for meaningful comparison, and estimates had to be made, often from illustrations of poorly oriented sections.

PRESENTATION OF DATA

An attempt has been made to illustrate the material as well as possible at magnifications of × 10 with selected details at × 50; thus the many attributes that cannot be adequately measured can be compared. The data obtained by measurement of the specimens are too voluminous to be included in the report, but they are available on request from the author. The data summaries at standard radii are presented. Tables 1–4 give some of the data and the rest are presented graphically on figures 2–9.

CORRELATION OF THE LOCAL SECTIONS

The samples studied from the four measured sections can be assigned relative positions even though sample localities are not directly connected. Locality 29 is isolated from more closely associated localities 30–32. The fauna of locality 29 is older than that of localities 31 or 32 and is probably younger than that of locality 30, but the evidence on this point is not conclusive. The fauna of locality 29 is not found between localities 30 and 31, but it may be present in the rocks forming the floor of Klawak Inlet. There is good correlation between localities 31 and 32, in spite of some uncertainties. Field data suggest that the section at locality 32 is a continuation of that at locality 31. It is possible, however, that the two sections overlap. The specimens of *Fusulinella alaskensis* n. sp. in sample f23979 from locality 31 are most similar to those from sample f23986 of locality 32. On the other hand, the only sample that yields *Beedeina*? sp. is f23986, the top sample at locality 32. This may indicate a slightly younger age for this sample.

The local section is represented by locality 30 at the base followed in ascending order by locality 29, locality 31 and locality 32. Localities 31 and 32 may overlap in part.

SYSTEMATIC DESCRIPTIONS

Genus TETRATAXIS Ehrenberg, 1854

Tetrataxis sp.

Plate 1, figures 1–3

Specimens referred to this genus are present in most samples used in this study. The examples illustrated are representative.

Genus BRADYINA von Möller, 1879

Bradyina sp.

Plate 4, figure 1

Fragmental specimens referred to this genus were recognized in several collections at localities 31 and 32. The example illustrated is representative.

Endothyrid, undet.

Plate 1, figures 4, 5

The specimens illustrated from locality 29 are assigned to the family Endothyridae. They may be the inner volutions of a larger form, but no large endothyrids were recognized in these samples.

Genus OZAWAINELLA Thompson, 1935

Ozawainella? sp.

Plate 4, figures 2, 3

The specimens referred with question to this genus show considerable resemblance to *Nankinella* sp. described below, but the wall is not recrystallized. The significance of the preservation is not understood, but is considered to involve the original wall material. The specimens from locality 31 are similar to those illustrated as *Ozawainella kurakhovensis* Manukalova (in Rauser-Chernoussova and others, 1951, p. 135) but the resemblance may be due primarily to the oblique way in which both specimens were cut.

Genus MILLERELLA Thompson, 1942

Millerella sp. aff. M. marblensis Thompson, 1942

Plate 2, figures 2, 3.

aff. *Millerella marblensis* Thompson, 1942, p. 405–407, pl. 1, figs. 3–14.

Discussion.—The specimens illustrated are representative of the *Millerella* found in sample f23975 in association with *Nankinella*, *Staffella*, and *Pseudostaffella*. The size, shape, and degree to which coiling is evolute fit well into the range reported by Thompson (1942, p. 405; 1948, p. 76).

Genus STAFFELLA Ozawa, 1925

Staffella sp. aff. S. powwowensis Thompson 1948

Plate 2, figure 1

aff. *Staffella powwowensis* Thompson, 1948, p. 78–79, pl. 25 fig. 7–12.

Discussion.—The specimen illustrated is closely similar to the specimen illustrated as figs. 10–11 on plate 25 by Thompson (1947) and is also apparently similar to the holotype, illustrated mostly as a drawing. Not enough is known about this genus for one to be able to distinguish species at the present time. The Alaskan specimen probably cannot be distinguished from the forms described from Powwow Canyon, Tex. The Texas form was found in association with *Millerella*, *Nankinella*, and *Profusulinella*. The Alaska form was found in sample f23975 with *Millerella*, *Nankinella*, and *Pseudostaffella*.

Genus NANKINELLA Lee, 1933

Nankinella sp.

Plate 1, figures 6–22

Diagnosis.—Small, discoidal, planispiral, with broadly angular periphery throughout and umbilicate axial regions. Wall structure indistinct, apparently with three layers.

Description.—The spiral form is normal negative to negative with the diameter increasing rapidly through the early stages and less rapidly near maturity. The shape is discoidal throughout with a broadly angular periphery and an umbilicate axis. The chamber height is greatest equatorially and diminishes gradually toward the axis. The form ratio increases gradually from around 0.44 in the inner volutions to about 0.5 in the outer volutions. The proloculus varies in size. The few specimens cut through the proloculus show a range from about 60 to 100 microns, but smaller prolocular diameters are suggested in some of the sections.

The wall structure is indistinct and is probably recrystallized. In some specimens the wall appears to be composed of two dark layers with a lighter layer in between. In other sections it seems to have one dark layer with lighter layers above and below. The thickness is difficult to determine, as the wall is irregular and indistinct.

The septa are unfluted, closely spaced, and inclined anteriorly. The tunnel occupies most of the equatorial peripheral area of each volution. Parachomata are developed at each septum but they do not join to form true chomata.

Comparisons and remarks.—The small number of specimens available for this study precludes satisfactory description or comparison with other members of the genus. Unfortunately no species in this genus has been adequately described. The forms from Alaska resemble *N. plummeri* Thompson (1947, p. 155) from the Marble Falls Limestone of Texas and *N.* spp. of Thompson, Pitrat, and Sanderson (1953, p. 547) from central British Columbia. The Alaskan forms are more tightly coiled than the Texas or Columbia forms, but one cannot assess the significance of this without knowing the limits of variability in the described forms.

419-577 O - 71 - 2

Distribution.—*Nankinella* sp. is associated with *Fusulinella pinguis* n. sp. in samples f23973 and f23974. Other associated forms include *Tetrataxis* sp. (pl. 1, figs. 1, 2) and endothyrids (pl. 1, figs. 4, 5). Rare specimens of *Nankinella* sp. are noted in f23975 associated with *Millerella* sp., *Staffella* sp., and *Pseudostaffella rotunda* n. sp.

Genus PSEUDOSTAFFELLA Thompson, 1942

Pseudostaffella rotunda n. sp.

Plate 2, figures 4–21

Diagnosis.—Shell small, globular with slightly umbilicate poles, the first 1–2 whorls at right angles to later whorls, septa plane, chomata relatively small and asymmetrical.

Description.—Summaries of the numerical data are given in table 1. The spiral form is negative to normal negative (fig. 2) with a tendency for an individual to increase in diameter rapidly at first and to grow less rapidly in the later stages. This is also expressed in figure 3 which shows the increase in volution height to be regularly arithmetic throughout most of the growth.

The length increases slowly relative to the radius (fig. 3). Note how closely similar the specimens are in this attribute. The form ratio increases in the early stages of growth and then gradually decreases (fig. 3). Individual specimens may develop a maximum form ratio of 1, but the mean form ratio is always less than 1.

Coiling starts in one plane but after 1 to 1½ volutions the axis rotates approximately 90° so that the third and subsequent volutions are at right angles to the juvenarium.

The proloculus ranges in outer diameter from 30 to 75 microns (fig. 3) with most specimens falling in the range of 50–60 microns.

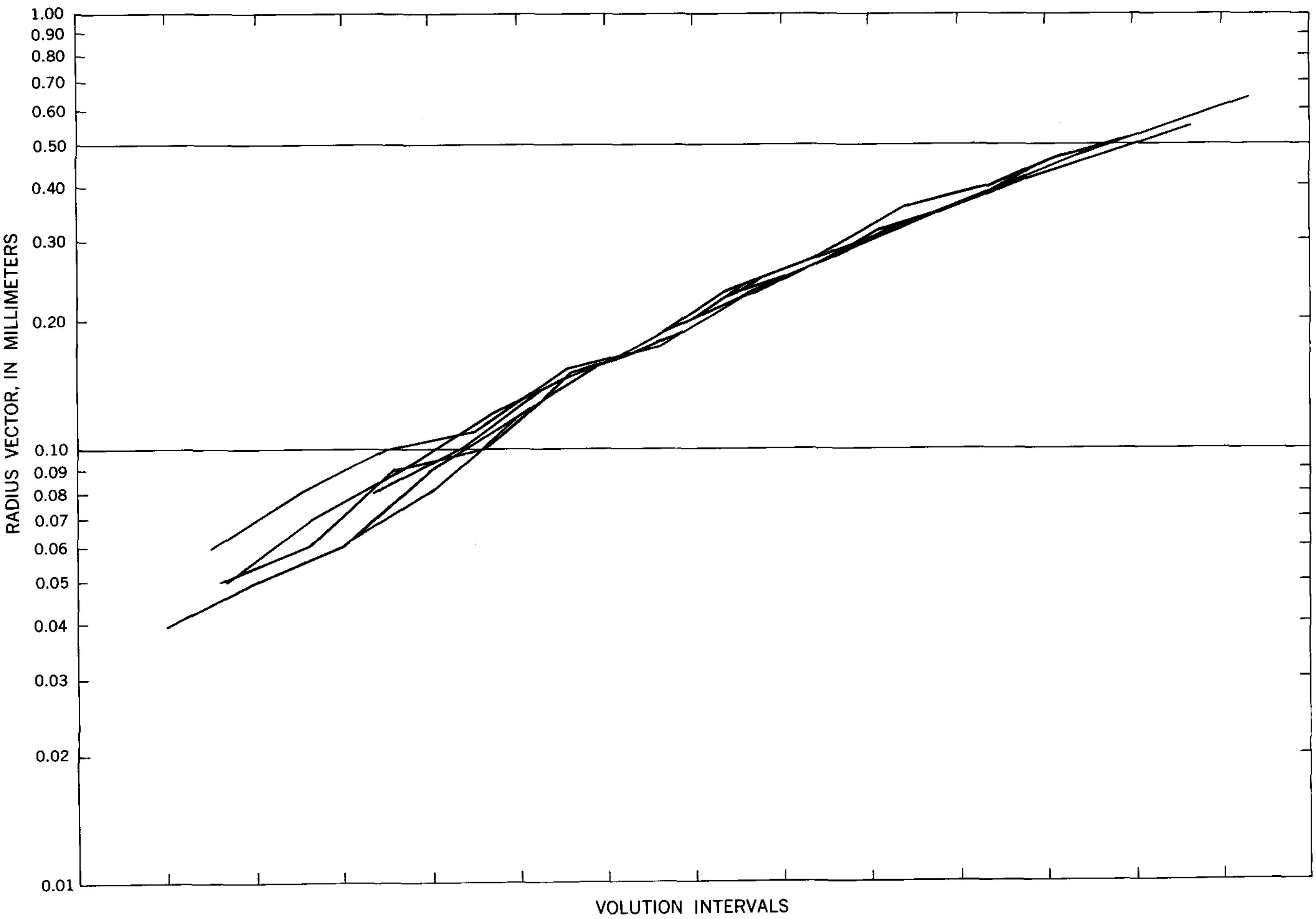

FIGURE 2.—The spiral form of *Pseudostaffella rotunda* n. sp. shown by a plot of radius vector on a logarithmic scale against volution intervals on an arithmetic scale. Six specimens from samples f23975 and f23976 are represented.

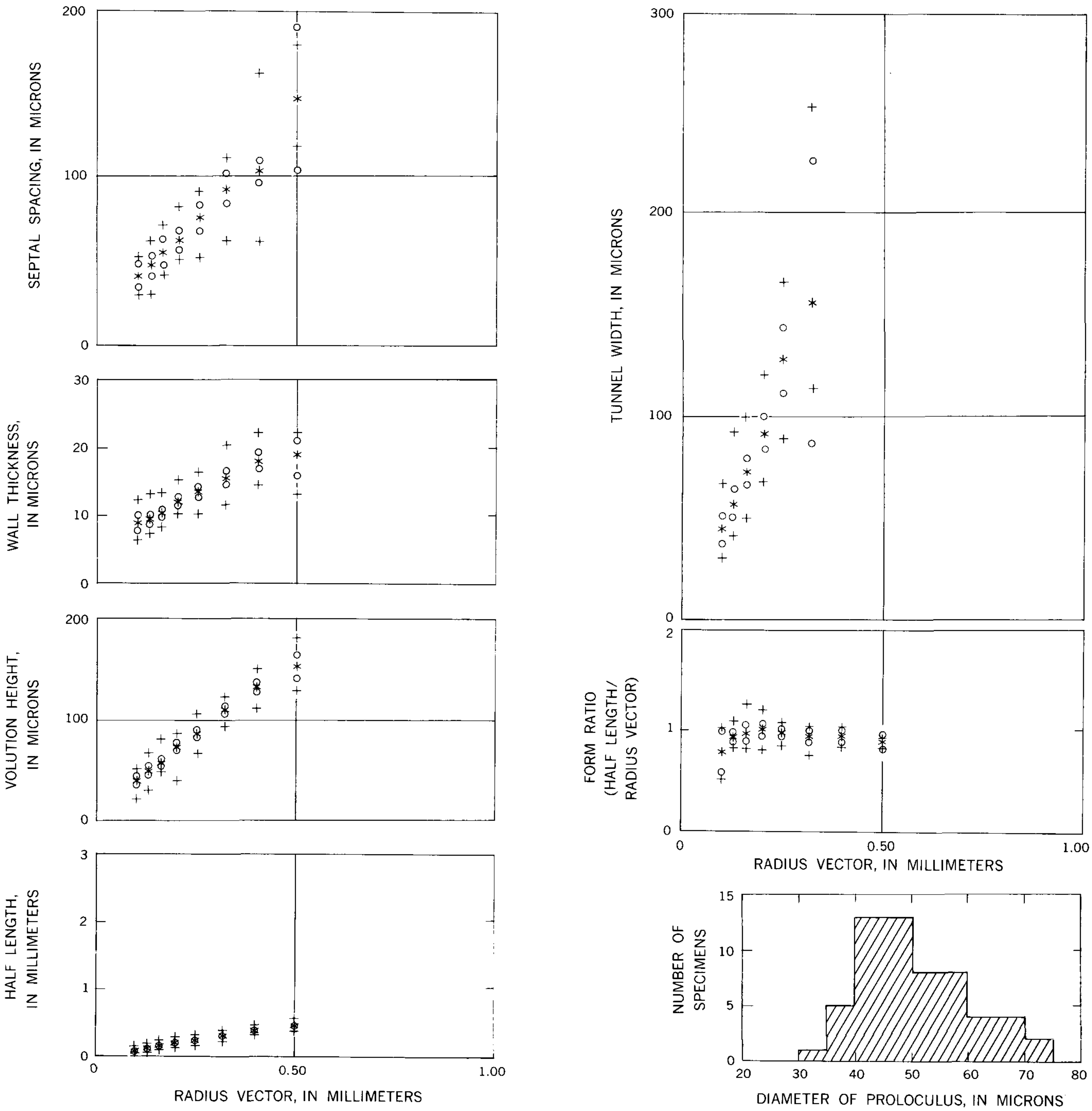

FIGURE 3.—Summary graphs for *Pseudostaffella rotunda* n. sp. The half length, volution height, wall thickness, septal spacing, form ratio, and tunnel width are plotted against radius vector. This shows the changes for each character during the ontogeny. The mean (*), confidence limits on the mean (o–o), and maximum and minimum (+–+) are shown at each standard radius. The numerical values for the means and confidence limits and the number of specimens on which they are based are given in table 1. The diameters of proloculi are plotted against the number of specimens.

TABLE 1.—*Summary numerical data for* Pseudostaffella rotunda *n. sp.*

[The data are presented at standard radii. All numbers are expressed in exponential notation. The number of digits recorded does not imply degree of accuracy]

Character	Number of specimens	Mean	Variance	Standard deviation	Coefficient of variability	Standard error of the mean
Radius vector	35	1.000E−01				
Half length	6	7.833E−02	3.767E−04	1.941E−02	2.478E+01	7.923E−03
Volution height	35	3.934E−02	6.253E−05	7.907E−03	2.010E+01	1.337E−03
Wall thickness	12	8.750E−03	2.386E−06	1.545E−03	1.765E+01	4.459E−04
Tunnel width	11	4.400E+01	1.068E+02	1.033E+01	2.349E+01	3.116E+00
Septal spacing	10	4.000E+00	4.444E−01	6.667E−01	1.667E+01	2.108E−01
Half length/radius vector	6	7.833E−01	3.767E−02	1.941E−01	2.478E+01	7.923E−02
Radius vector	35	1.305E−01				
Half length	8	1.175E−01	1.071E−04	1.035E−02	8.809E+00	3.660E−03
Volution height	35	4.943E−02	6.161E−05	7.849E−03	1.588E+01	1.327E−03
Wall thickness	26	9.192E−03	1.762E−06	1.326E−03	1.444E+01	2.603E−04
Tunnel width	15	5.680E+01	1.467E+02	1.211E+01	2.133E+01	3.128E+00
Septal spacing	15	4.667E+00	8.095E−01	8.997E−01	1.928E+01	2.323E−01
Half length/radius vector	8	9.038E−01	6.340E−03	7.962E−02	8.809E+00	2.815E−02
Radius vector	36	1.600E−01				
Half length	13	1.554E−01	3.603E−04	1.898E−02	1.222E+01	5.264E−03
Volution height	35	5.757E−02	5.296E−05	7.277E−03	1.264E+01	1.230E−03
Wall thickness	32	9.969E−03	1.386E−06	1.177E−03	1.181E+01	2.081E−04
Tunnel width	16	7.200E+01	1.404E+02	1.185E+01	1.646E+01	2.962E+00
Septal spacing	17	5.412E+00	1.007E+00	1.004E+00	1.855E+01	2.434E−01
Half length/radius vector	13	9.712E−01	1.407E−02	1.186E−01	1.222E+01	3.290E−02
Radius vector	36	2.000E−01				
Half length	14	1.979E−01	4.643E−04	2.155E−02	1.089E+01	5.759E−03
Volution height	36	7.267E−02	7.183E−05	8.475E−03	1.166E+01	1.413E−03
Wall thickness	35	1.169E−02	2.987E−06	1.728E−03	1.479E+01	2.921E−04
Tunnel width	15	9.140E+01	2.178E+02	1.476E+01	1.615E+01	3.811E+00
Septal spacing	19	6.211E+00	6.199E−01	7.873E−01	1.268E+01	1.806E−01
Half length/radius vector	14	9.893E−01	1.161E−02	1.077E−01	1.089E+01	2.879E−02
Radius vector	36	2.500E−01				
Half length	14	2.429E−01	2.989E−04	1.729E−02	7.119E+00	4.621E−03
Volution height	36	8.656E−02	6.443E−05	8.027E−03	9.273E+00	1.338E−03
Wall thickness	35	1.320E−02	3.165E−05	1.779E−03	1.348E+01	3.007E−04
Tunnel width	11	1.277E+02	5.972E+02	2.444E+01	1.913E+01	7.368E+00
Septal spacing	20	7.500E+00	1.316E+00	1.147E+00	1.529E+01	2.565E−01
Half length/radius vector	14	9.714E−01	4.782E−03	6.916E−02	7.119E+00	1.848E−02
Radius vector	33	3.200E−01				
Half length	13	2.969E−01	5.731E−04	2.394E−02	3.062E+00	6.639E−03
Volution height	33	1.082E−01	6.600E−05	8.124E−03	7.506E+00	1.414E−03
Wall thickness	32	1.519E−02	5.319E−06	2.305E−03	1.513E+01	4.077E−04
Tunnel width	5	1.564E+02	3.173E+03	5.633E+01	3.602E+01	2.519E+01
Septal spacing	18	9.222E+00	2.065E+00	1.437E+00	1.558E+01	3.387E−01
Half length/radius vector	13	9.279E−01	5.596E−03	7.481E−02	8.062E+00	2.075E−02
Radius vector	22	4.000E−01				
Half length	8	3.725E−01	5.929E−04	2.435E−02	6.537E+00	8.609E−03
Volution height	22	1.306E−01	1.099E−04	1.048E−02	8.023E+00	2.235E−03
Wall thickness	22	1.759E−02	5.968E−06	2.443E−03	1.389E+01	5.208E−04
Septal spacing	12	1.108E+01	7.720E+00	2.778E+00	2.507E+01	8.021E−01
Half length/radius vector	8	9.312E−01	3.705E−03	6.087E−02	6.537E+00	2.152E−02
Radius vector	9	5.000E−01				
Half length	3	4.533E−01	2.333E−04	1.528E−02	3.370E+00	8.819E−03
Volution height	9	1.512E−01	2.327E−04	1.525E−02	1.009E+01	5.085E−03
Wall thickness	8	1.837E−02	1.055E−05	3.249E−03	1.768E+01	1.149E−03
Septal spacing	4	1.475E+01	7.583E+00	2.754E+00	1.867E+01	1.377E+00
Half length/radius vector	3	9.067E−01	9.333E−04	3.055E−02	3.370E+00	1.764E−02

The character of the wall is not altogether clear. In some parts of the shell it is composed of tectum and diaphanotheca alone, but in other parts tectoria are developed. The wall thickness (fig. 3) increases gradually from about 9 microns to just over 20 microns. These measurements taken on equatorial sections are of tectum and diaphanotheca. The tectoria are generally restricted to the vicinity of the septa.

The septa are plane. The septal spacing increases arithmetically to about 150 microns in large specimens (fig. 3). The spacing is not regular, however, and the last few chambers are commonly widely spaced. The septa thicken toward their bases in the vicinity of the tunnel.

The tunnel is well defined and generally less than half the volution height. The width is variable (fig. 3) and tends to increase rapidly. It is bounded by relatively small asymmetrical chomata that may appear large in some sections where they coincide with the septal plane.

Comparisons and remarks.—These specimens belong to a group of medium-sized Pseudostaffellas intermediate in character between *Pseudostaffella antiqua* (Dutkevich) and *P. sphaeroidea* (Möller). They differ from *P. antiqua* in being larger and possibly in regularity of coiling. Unfortunately, orientation of sections is a problem with these forms; hence, it is difficult to make comparisons based on the published data. Closely similar forms include the following: *P.* cf. *P. antiqua* (Dutkevich) of Forbes 1960 from the lower part of the Passage Beds in Spitsbergen; the specimens described by Forbes have smaller proloculi, do not attain the size of the Alaska specimens, and have smaller chomata.

P. kanumai Igo, 1957 from the lowest part of the Ichinotani Formation in central Japan; the specimens described are a little smaller and have a larger form ratio than those from Alaska. *P. sandersoni* Thompson, 1965 from the Fort St. James area in British Columbia, Canada; the specimens described by Thompson are smaller, less regularly coiled, and less round than the specimens from Alaska.

Material studied.—The description and illustrations are based on samples f23975 and f23976 in which *Pseudostaffella* is common and is associated with rare *Millerella*, *Nankinella*, *Staffella* sp., and possible *Climacammina* sp. Thirty-six oriented sections were measured, and many other specimens in 60 thin sections were used to describe this species. No larger fusulinids were found in the section sampled on Peratovich Island.

Designation of types.—The specimen illustrated on plate 2 as figures 4a and 4b is designated the holotype. The other specimens studied are paratypes.

Genus **FUSULINELLA** Möller, 1877

Fusulinella pinguis n. sp.

Plate 3, figures 1–28

Diagnosis.—Shell small, attaining lengths around 2.5 mm and widths around 1.5 mm in about five volutions. The shape is inflated fusiform with convex to concave lateral slopes and bluntly pointed poles. The coiling is relatively loose and the septa nearly straight with some secondary deposits extending poleward from the chomata.

Description.—Summaries of the numerical data are given in table 2. The spiral form is normal to normal negative, with a tendency to be positive in the early stages so that the whole curve is weekly sigmoidal (fig. 4). The diameter increase is shown in the plots for height of volution (fig. 5) and it is apparent that the height increases rapidly in the inner volutions and then increases less rapidly in the outer volutions.

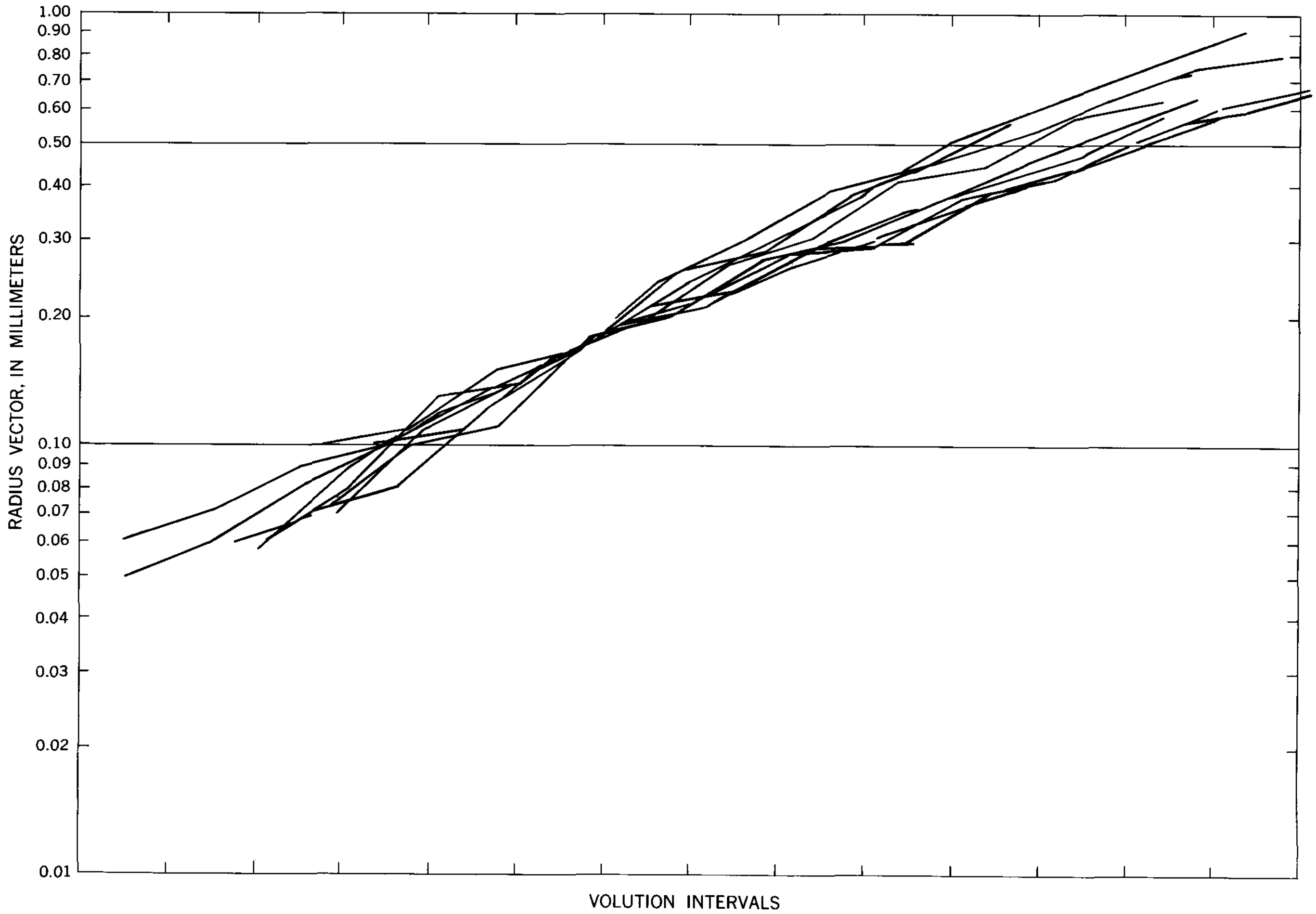

FIGURE D.—The spiral form of *Fusulinella pinguis* n. sp. shown by a plot of radius vector on a logarithmic scale against volution intervals on an arithmetic scale. Nine specimens from samples f23973 and f23974 are represented.

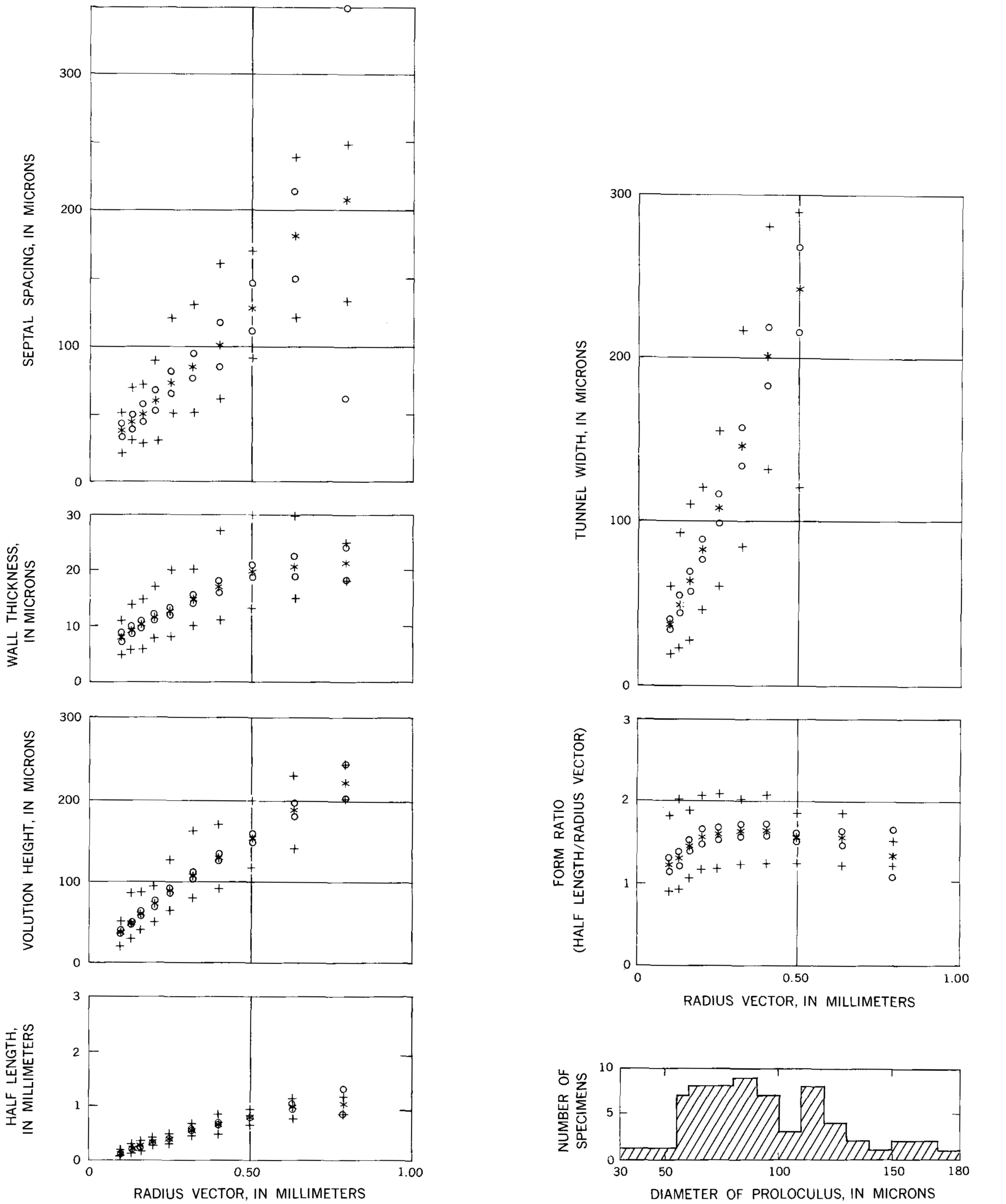

FIGURE 5.—Summary graphs for *Fusulinella pinguis* n. sp. The half length, volution height, wall thickness, septal spacing, form ratio, and tunnel width are each plotted against the radius vector. This shows the changes for each character during the ontogeny. The mean (*), confidence limits on the mean (o–o), and maximum and minimum (+–+) are shown at each standard radius. The numerical values for the means and confidence limits and the number of specimens on which each is based are given in table 2. The diameters of proloculi are plotted against the number of specimens.

TABLE 2.—*Summary numerical data for* Fusulinella pinguis *n. sp.*

[The data are presented at standard radii. All numbers are expressed in exponential notation. The number of digits recorded does not imply degree of accuracy.]

Character	Number of specimens	Mean	Variance	Standard deviation	Coefficient of variability	Standard error of the mean
Radius vector	56	1.000E-01				
Half length	34	1.215E-01	5.584E-04	2.363E-02	1.945E+01	4.053E-03
Volution height	56	3.757E-02	4.112E-05	6.413E-03	1.707E+01	8.569E-04
Wall thickness	22	8.091E-03	2.944E-06	1.716E-03	2.121E+01	3.658E-04
Tunnel width	31	3.729E+01	7.048E+01	8.395E+00	2.251E+01	1.508E+00
Septal spacing	21	3.667E+00	9.333E-01	9.661E-01	2.635E+01	2.108E-01
Half length/radius vector	34	1.215E+00	5.584E-02	2.363E-01	1.945E+01	4.053E-02
Radius vector	63	1.300E-01				
Half length	39	1.667E-01	1.186E-03	3.444E-02	2.066E+01	5.514E-03
Volution height	63	4.784E-02	6.336E-05	7.960E-03	1.664E+01	1.003E-03
Wall thickness	36	9.306E-03	2.447E-06	1.564E-03	1.681E+01	2.607E-04
Tunnel width	37	4.951E+01	2.330E+02	1.527E+01	3.083E+01	2.510E+00
Septal spacing	24	4.292E+00	1.433E+00	1.197E+00	2.789E+01	2.444E-01
Half length/radius vector	39	1.282E+00	7.018E-02	2.649E-01	2.066E+01	4.242E-02
Radius vector	64	1.600E-01				
Half length	39	2.297E-01	1.282E-03	3.580E-02	1.558E+01	5.732E-03
Volution height	64	5.758E-02	6.025E-05	7.762E-03	1.348E+01	9.702E-04
Wall thickness	52	1.029E-02	2.327E-06	1.525E-03	1.483E+01	2.115E-04
Tunnel width	37	6.297E+01	2.884E+02	1.698E+01	2.697E+01	2.792E+00
Septal spacing	25	5.040E+00	9.567E-01	9.781E-01	1.941E+01	1.956E-01
Half length/radius vector	39	1.436E+00	5.006E-02	2.237E-01	1.558E+01	3.583E-02
Radius vector	64	2.000E-01				
Half length	39	3.105E-01	2.252E-03	4.746E-02	1.528E+01	7.600E-03
Volution height	64	7.023E-02	1.099E-04	1.048E-02	1.493E+01	1.311E-03
Wall thickness	60	1.140E-02	3.566E-06	1.888E-03	1.657E+01	2.438__-04
Tunnel width	37	8.235E+01	3.287E+02	1.813E+01	2.201E+01	2.980E+00
Septal spacing	25	6.000E+00	2.083E+00	1.443E+00	2.406E+01	2.887E-01
Half length/radius vector	39	1.553E+00	5.631E-02	2.373E-01	1.528E+01	3.800E-02
Radius vector	64	2.500E-01				
Half length	39	3.990E-01	2.662E-03	5.160E-02	1.293E+01	8.262E-03
Volution height	64	8.777E-02	1.348E-04	1.161E-02	1.323E+01	1.452E-03
Wall t hickness	64	1.269E-02	7.004E-06	2.654E-03	2.092E+01	3.317E-04
Tunnel width	35	1.069E+02	6.448E+02	2.539E+01	2.374E+01	4.292E+00
Septal spacing	25	7.440E+00	2.757E+00	1.660E+00	2.232E+01	3.321E-01
Half length/radius vector	39	1.596E+00	4.259E-02	2.064E-01	1.293E+01	3.305E-02
Radius vector	64	3.200E-01				
Half length	39	5.218E-01	4.157E-03	6.448E-02	1.236E+01	1.032E-02
Volution height	64	1.045E-01	2.389E-04	1.546E-02	1.479E+01	1.932E-03
Wall thickness	64	1.473E-02	7.881E-06	2.807E-03	1.905E+01	3.509E-04
Tunnel width	30	1.455E+02	9.896E+02	3.146E+01	2.162E+01	5.743E+00
Septal spacing	25	8.560E+00	3.757E+00	1.938E+00	2.264E+01	3.876E-01
Half length/radius vector	39	1.631E+00	4.060E-02	2.015E-01	1.236E+01	3.226E-02
Radius vector	58	4.000E-01				
Half length	36	6.522E-01	5.841E-03	7.642E-02	1.172E+01	1.274E-02
Volution height	58	1.267E-01	2.676E-04	1.636E-02	1.291E+01	2.148E-03
Wall thickness	58	1.698E-02	1.167E-05	3.416E-03	2.011E+01	4.485E-04
Tunnel width	23	2.011E+02	1.555E+03	3.943E+01	1.961E+01	8.222E+00
Septal spacing	22	1.009E+01	5.610E+00	2.369E+00	2.347E+01	5.050E-01
Half length/radius vector	36	1.631E+00	3.650E-02	1.911E-01	1.172E+01	3.184E-02
Radius vector	51	5.000E-01				
Half length	31	7.761E-01	4.651E-03	6.820E-02	8.787E+00	1.225E-02
Volution height	51	1.534E-01	3.034E-04	1.742E-02	1.136E+01	2.439F-03
Wall thickness	49	1.973E-02	1.499E-05	3.872E-03	1.962E+01	5.533E-04
Tunnel width	14	2.412E+02	2.072E+03	4.551E+01	1.887E+01	1.216E+01
Septal spacing	19	1.284E+01	5.251E+00	2.292E+00	1.784E+01	5.257E-01
Half length/radius vector	31	1.552E+00	1.860E-02	1.364E-01	8.787E+00	2.450E-02
Radius vector	29	6.300E-01				
Half length	17	9.629E-01	8.960E-03	9.465E-02	9.830E+00	2.296E-02
Volution height	28	1.856E-01	4.089E-04	2.022E-02	1.089E+01	3.822E-03
Wall thickness	26	2.058E-02	2.097E-05	4.580E-03	2.226E+01	8.982E-04
Septal spacing	12	1.808E+01	1.154E+01	3.397E+00	1.878E+01	9.806E-01
Half length/radius vector	17	1.528E+00	2.257E-02	1.502E-01	9.830E+00	3.644E-02
Radius vector	6	7.900E-01				
Half length	3	1.063E+00	8.533E-03	9.238E-02	8.687E+00	5.333E-02
Volution height	6	2.197E-01	4.103E-04	2.026E-02	9.221E+00	8.269E-03
Wall thickness	6	2.117E-02	9.367E-06	3.061E-03	1.446E+01	1.249E-03
Septal spacing	3	2.067E+01	3.433E+01	5.859E+00	2.835E+01	3.383E+00
Half length/radius vector	3	1.346E+00	1.367E-02	1.169E-01	8.687E+00	6.751E-02

The length increases logarithmically in relation to the diameter in the smaller part of the test; it increases more slowly in the larger parts (fig. 5). The plot of the form ratio at various radii (fig. 5) shows the rapid increase and then gradual decrease during growth.

The proloculus ranges in outer diameter from about 30 to 180 microns with most specimens fairly evenly distributed in the 60–120 micron range and only 14 specimens falling outside that range (fig. 5). A few microspheric forms were found.

The wall thickness in the small parts of the shell increases regularly and arithmetically in relation to the radius; it increases less rapidly after specimens attain a radius of about half a millimeter (fig. 5). The maximum thickness recorded was 30 microns. The measurements were all made in the equatorial area and did not include secondary deposits of the kind shown in fig. 17b, pl. 3. The wall appears to thin toward the poles, but no measurements were made. The wall has a tectum, a well-defined diaphanotheca, and generally a well-defined thin inner tectorium. Development of an outer tectorium or other secondary deposits is discontinuous and commonly confined to areas at the base of the septa.

The septa are plane or only slightly fluted toward the poles. They are spaced rather regularly, and the spacing tends to increase arithmetically with increasing radius (fig. 5). The septa tend to thicken in the vicinity of the tunnel.

The tunnel is well defined and generally about half the height of the volution. It increases rapidly in width with increasing radius (fig. 5) and is bounded by asymmetrical chomata that may overhang the tunnel. The distinction between chomata, as such, and thickening of the septa in the tunnel area is not clear. Where the plane septa are intercepted by the section (pl. 3, figs. 6b, 27) there is a suggestion of axial filling, but this is not true axial filling.

Comparisons and remarks.—*Fusulinella pinguis* n. sp. is similar in many respects to the general group of *F. bocki* Möller, 1878. The size and shape, the generally straight septa, the narrow tunnel with well-developed chomata, and the wall structure all lend similarity to the general group that includes at least the following named forms: *F. bocki* Möller 1878, p. 104; *F. bocki timanica* Rauser 1951, p. 224 (in Rauser-Cherroussova and others, 1951); *F. jamesensis* Thompson, Pitrat, and Sanderson 1953, p. 548; *F. simplicata* Toriyama 1958, p. 36; *F. simplicata simplicata* Toriyama of Ishii 1962, p. 15; *F. pygmaea* Ishii 1962, p. 19; *F. bocki bocki* Möller of Ishii 1962, p. 22; *F. bocki rotunda* Ishii 1962, p. 24; *F. bocki biconiformis* Ishii 1962, p. 25; *F. pandae* Ginkel 1965, p. 149; *F. maldrigensis* Ginkel 1965, p. 150; *F.* ex gr *bocki* Möller of Ginkel 1965, p. 159; and *F. alaskensis* n. sp. described below.

Numerical data for a detailed comparison are available for some of the forms within this group. Using these data, the author made interpolations to facilitate comparisons at standard radii. The wall thickness of *F. pinguis* is consistently thinner than that of any of the above forms with no overlap in the outer volutions of most specimens. The most similar form in this respect is *F. pygmaea* Ishii in which, although the wall is consistently thicker, there is some overlap in the total range of thickness.

The form ratio (half length/radius vector) in *F. pinguis* is smaller than for most of this group. The specimens described by Ishii 1962 as *F. bocki bocki*, *F. b. rotunda*, and *F. b. biconiformis* have a smaller mean form ratio than *F. pinguis* with some overlap in the total range. The greatest similarity in all characters studied is to *F. bocki bocki* of Ishii, but the greater wall thickness in that form distinguishes it without difficulty. Comparisons with *F. alaskensis* n. sp. are given under that species.

Material studied.—*F. pinguis* n. sp. is common in samples f23973 and f23974 at locality 29 where it is associated with *Tetrataxis* sp., endothyrids, and *Nankinella* sp. Sixty-four oriented sections were measured, and many other specimens in 91 thin sections were used to describe this species.

Designation of types.—The specimen illustrated on plate 3 as figures 1a–b designated the holotype. The other specimens studied are paratypes.

Fusulinella alaskensis n. sp.

Plate 4, figures 4–30; Plate 5, figures 1–8; Plate 6, figures 1–15

Diagnosis.—Shell small, attaining lengths around 4 mm and widths around 2 mm in about 6 volutions. The shape is fusiform with irregular to concave lateral slopes and bluntly pointed poles. The coiling is relatively loose and the chambers relatively open with little secondary filling and small chomata.

Description.—Summaries of the numerical data are given in table 3. The spiral form is normal to normal negative increasing regularly through the early volutions and increasing only slightly less in the outer volutions (fig. 6.). The pattern for the increase in height of volution for combined samples of this species is shown in figure 7 where it is seen that the increase is quite regular throughout most of the growth.

The length increases logarithmically in relation to the diameter. Figure 7 shows a straight-line plot of log half lengths against radius vector. Note that the spread is narrow throughout, indicating a close homogeneity in specimens from the seven samples.

The form ratio increases rapidly in the early stages of growth and then remains almost constant (fig. 7). The shape is fusiform throughout, with a tendency to develop concave lateral slopes even in some of the early volutions.

The proloculus ranges in outer diameter from about 50 to 130 microns in the megalospheric specimens. More than a third of the specimens are in the 75 to 90 micron range (fig. 7), and the rest fall about equally to each side of this central cluster. Several microspheric juvenaria were found with proloculi about 25 microns in diameter. Some specimens with larger proloculi seem intermediate in form with the initial chambers at an angle to the adult chambers (pl. 5, fig. 3, 8).

The wall thickness increases regularly as shown in figure 7. The maximum thickness recorded was 32 microns. All measurements were taken from the equatorial

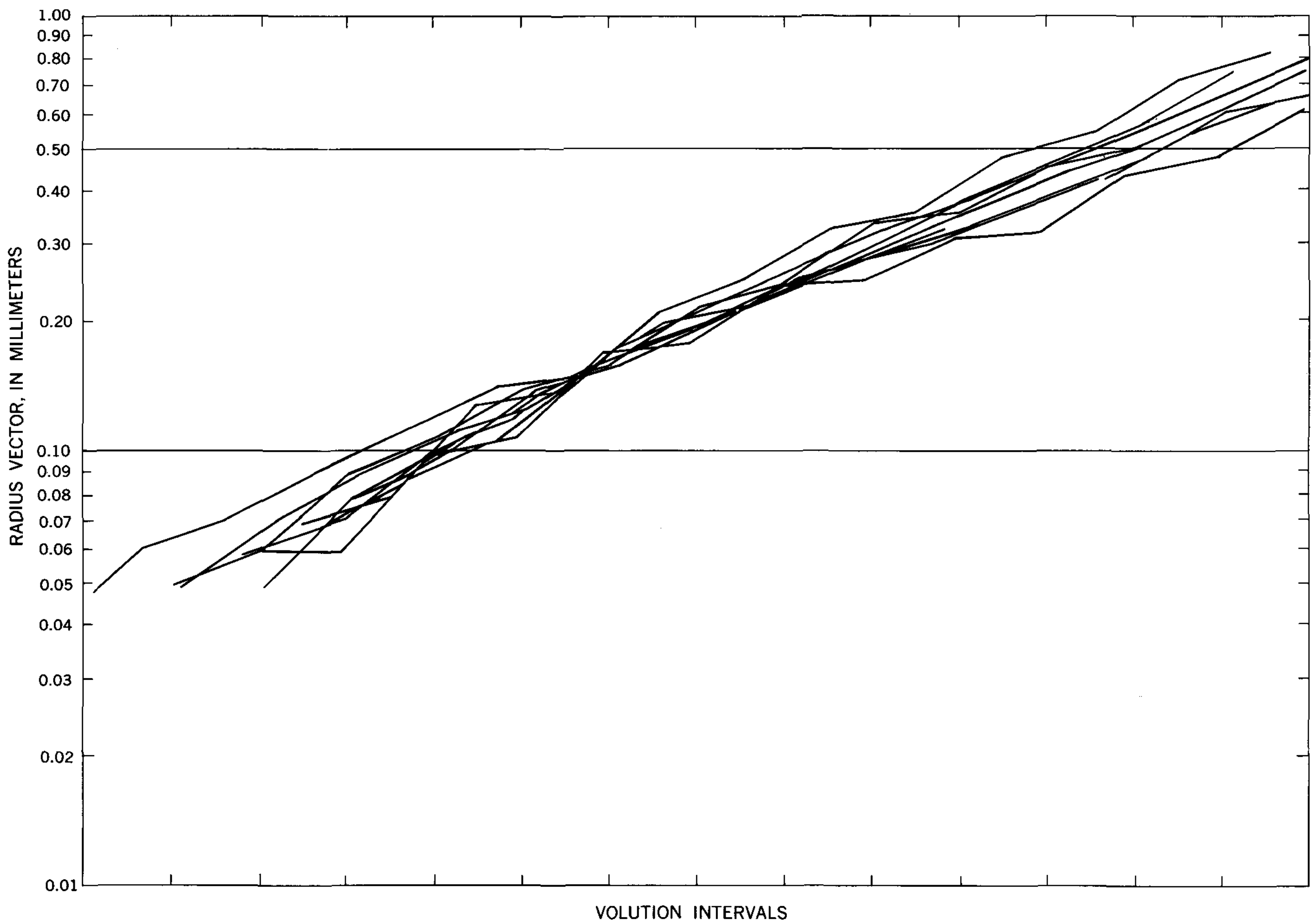

FIGURE 6.—The spiral form of *Fusulinella alaskensis* n. sp. shown by a plot of radius vector on a logarithmic scale against volution intervals on an arithmetic scale. Ten specimens from samples f23977, f23979, and f23986 are represented.

area and, although the wall appears to thin gradually toward the poles no measurements were taken in that area. The wall has a tectum and well-defined diaphanotheca (pl. 5) and thin, irregular tectoria, mostly in the vicinity of the septa.

The septa tend to be plane or slightly fluted and are spaced rather regularly throughout most of the shell. The septal spacing increases arithmetically with increasing radius (fig. 7). The septa are thickened to wedges or bulbs by secondary deposits in the vicinity of the tunnel and chomata.

The tunnel is well defined by the chomata. It is generally low, extending less than half the height of the chambers. It tends to be straight or only slightly irregular and increases rapidly in width (fig. 7.). The bounding chomata are small and tend to be symmetrical. Where the plane of the septa coincides or nearly coincides with the plane at the section, the chomata appear to be more massive and asymmetrical because of the extension of secondary deposits along the septa (pl. 5. figs. 1, 2, 6).

Comparisons and remarks.—*Fusulinella alaskensis* n. sp. somewhat resembles the forms listed in the discussion of *F. pinguis* n. sp., but increases more rapidly in length than most of those forms and, therefore has a larger form ratio. One exception is *F. simplicata* Toriyama 1958, p. 36. The specimens measured by Toriyama have a large, though variable, form ratio, and the four specimens have a consistently higher mean than *F. alaskensis.* This is in contrast with the several subspecies of *F. simplicata* described by Ishii (1962) from Shikoku.

Other species with which *F. alaskensis* may be compared are: *F. iyoensis* Ishii 1962, p. 14, which has the same general shape but a thicker wall and smaller form ratio; *F. thompsoni* Skinner and Wilde 1954, p. 797, which has less concave lateral slopes, more strongly fluted septa, and a much thicker wall; and *F. peruana* Dunbar and Newell 1946, p. 486, which is similar to *F. thompsoni* but has a slightly larger form ratio and an even thicker wall at maturity. Comparison between *F. pinguis* n. sp. and *F. alaskensis* n. sp. shows that the

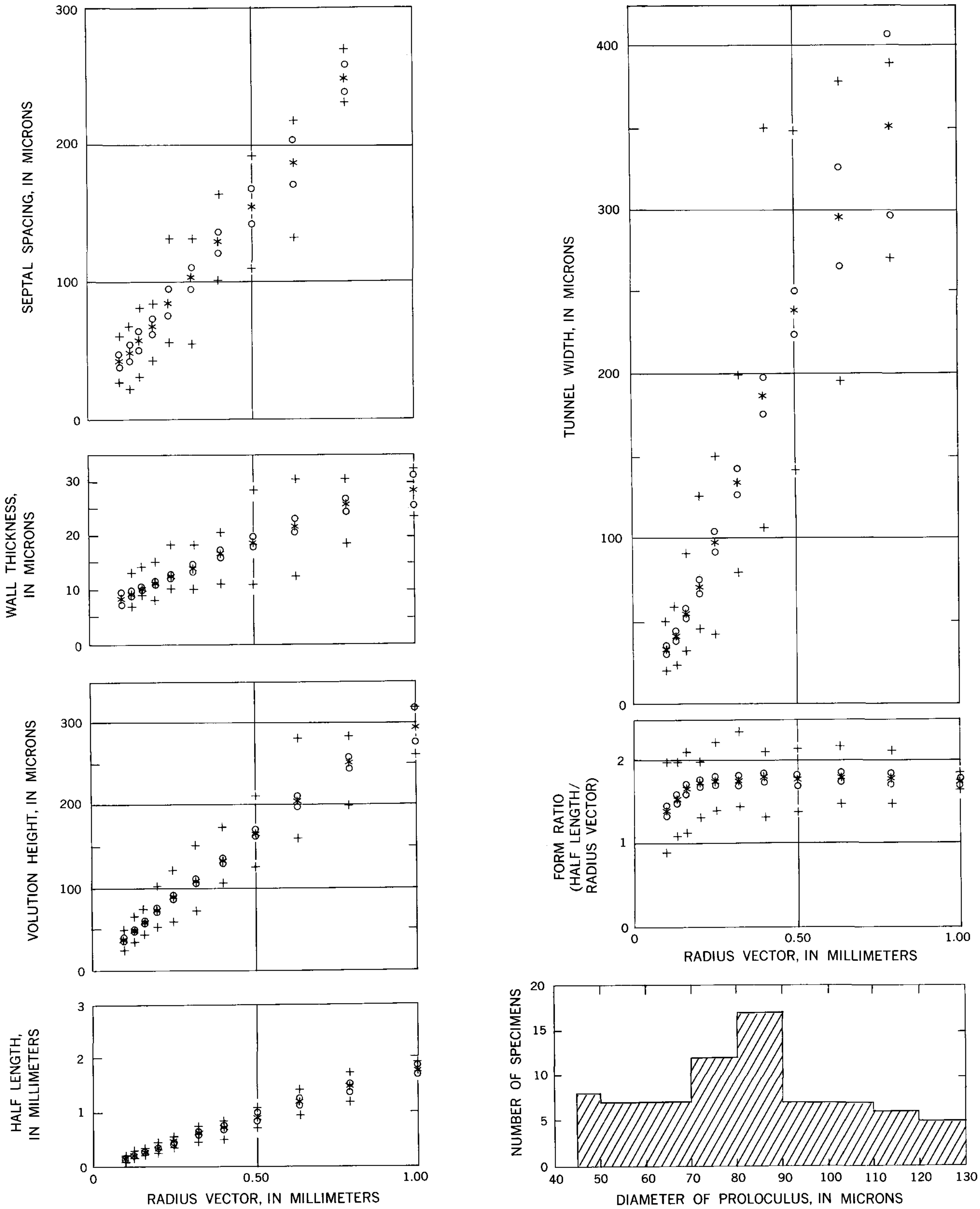

FIGURE 7.—Summary graphs for *Fusulinella alaskensis* n. sp. The half length, volution height, wall thickness, septal spacing form ratio, and tunnel width are each plotted against the radius vector. This shows the changes for each character during the ontogeny. The mean (*), confidence limits on the mean (O–O), and maximum and minimum (+–+) are shown at each standard radius. The numerical values for the means and confidence limits and the number of specimens on which each is based are given in table 3. The diameters of proloculi are plotted against the number of specimens.

TABLE 3.—*Summary numerical data for* Fusulinella alaskensis *n. sp.*

[The data are presented at standard radii. All numbers are expressed in exponential notation. The number of digits recorded does not imply degree of accuracy]

Character	Number of specimens	Mean	Variance	Standard deviation	Coefficient of variability	Standard error of the mean
Radius vector	77	1.000E−01				
Half length	60	1.408E−01	5.366E−04	2.316E−02	1.645E+01	2.990E−03
Volution height	77	3.800E−02	2.926E−05	5.410E−03	1.424E+01	6.165E−04
Wall thickness	5	8.400E−03	8.000E−07	8.944E−04	1.065E+01	4.000E−04
Tunnel width	60	3.255E+01	4.693E+01	6.851E+00	2.105E+01	8.844E−01
Septal spacing	17	4.212E+01	9.224E+01	9.604E+00	2.280E+01	2.329E+00
Half length/radius vector	60	1.408E+00	5.366E−02	2.316E−01	1.645E+01	2.990E−02
Radius vector	78	1.300E−01				
Half length	60	1.992E−01	7.129E−04	2.670E−02	1.341E+01	3.447E−03
Volution height	78	4.681E−02	3.330E−05	5.771E−03	1.233E+01	6.534E−04
Wall thickness	28	9.286E−03	1.545E−06	1.243E−03	1.339E+01	2.349E−04
Tunnel width	60	4.075E+01	8.636E+01	9.293E+00	2.280E+01	1.200E+00
Septal spacing	18	4.817E+01	1.364E+02	1.168E+01	2.425E+01	2.753E+00
Half length/radius vector	60	1.532E+00	4.218E−02	2.054E−01	1.341E+01	2.651E−02
Radius vector	78	1.600E−01				
Half length	60	2.653E−01	1.225E−03	3.500E−02	1.319E+01	4.519E−03
Volution height	78	5.709E−02	4.245E−05	6.515E−03	1.141E+01	7.377E−04
Wall thickness	48	1.015E−02	8.506E−07	9.223E−04	9.090E+00	1.331E−04
Tunnel width	60	5.413E+01	1.153E+02	1.074E+01	1.984E+01	1.386E+00
Septal spacing	18	5.683E+01	1.776E+02	1.333E+01	2.345E+01	3.141E+00
Half length/radius vector	60	1.658E+00	4.786E−02	2.188E−01	1.319E+01	2.824E−02
Radius vector	78	2.000E−01				
Half length	60	3.460E−01	1.007E−03	3.174E−02	9.174E+00	4.098E−03
Volution height	78	7.036E−02	6.361E−05	7.976E−03	1.134E+01	9.031E−04
Wall thickness	68	1.078E−02	1.607E−06	1.268E−03	1.176E+01	1.537E−04
Tunnel width	59	7.017E+01	2.302E+02	1.517E+01	2.162E+01	1.975E+00
Septal spacing	18	6.706E+01	1.159E+02	1.077E+01	1.606E+01	2.538E+00
Half length/radius vector	60	1.730E+00	2.519E−02	1.587E−01	9.174E+00	2.049E−02
Radius vector	77	2.500E−01				
Half length	60	4.400E−01	1.932E−03	4.396E−02	9.990E+00	5.675E−03
Volution height	77	8.630E−02	8.361E−05	9.144E−03	1.060E+01	1.042E−03
Wall thickness	77	1.206E−02	2.588E−06	1.609E−03	1.333E+01	1.833E−04
Tunnel width	58	9.690E+01	5.017E+02	2.240E+01	2.312E+01	2.941E+00
Septal spacing	17	8.382E+01	3.418E+02	1.849E+01	2.205E+01	4.484E+00
Half length/radius vector	60	1.760E+00	3.092E−02	1.758E−01	9.990E+00	2.270E−02
Radius vector	77	3.200E−01				
Half length	60	5.657E−01	3.296E−03	5.741E−02	1.015E+01	7.412E−03
Volution height	77	1.054E−01	1.838E−04	1.356E−02	1.286E+01	1.545E−03
Wall thickness	76	1.376E−02	5.276E−06	2.297E−03	1.669E+01	2.635E−04
Tunnel width	57	1.333E+02	8.891E+02	2.982E+01	2.237E+01	3.949E+00
Septal spacing	17	1.017E+02	2.442E+02	1.563E+01	1.537E+01	3.790E+00
Half length/radius vector	60	1.768E+00	3.219E−02	1.794E−01	1.015E+01	2.316E−02
Radius vector	73	4.000E−01				
Half length	57	7.195E−01	5.259E−03	7.252E−02	1.008E+01	9.605E−03
Volution height	73	1.306E−01	1.695E−04	1.302E−02	9.970E+00	1.524E−03
Wall thickness	73	1.621E−02	6.054E−06	2.461E−03	1.518E+01	2.880E−04
Tunnel width	53	1.867E+02	1.758E+03	4.193E+01	2.245E+01	5.759E+00
Septal spacing	15	1.273E+02	1.987E+02	1.409E+01	1.107E+01	3.639E+00
Half length/radius vector	57	1.799E+00	3.287E−02	1.813E−01	1.008E+01	2.401E−02
Radius vector	70	5.000E−01				
Half length	56	8.905E−01	8.154E−03	9.030E−02	1.014E+01	1.207E−02
Volution height	70	1.630E−01	2.522E−04	1.588E−02	9.743E+00	1.898E−03
Wall thickness	70	1.841E−02	9.956E−06	3.155E−03	1.714E+01	3.771E−04
Tunnel width	40	2.376E+02	1.627E+03	4.034E+01	1.697E+01	6.378E+00
Septal spacing	14	1.556E+02	4.827E+02	2.197E+01	1.412E+01	5.872E+00
Half length/radius vector	56	1.781E+00	3.262E−02	1.806E−01	1.014E+01	2.413E−02
Radius vector	59	6.300E−01				
Half length	46	1.143E+00	1.492E−02	1.221E−01	1.068E+01	1.801E−02
Volution height	59	2.029E−01	4.500E−04	2.121E−02	1.045E+01	2.762E−03
Wall thickness	57	2.116E−02	1.521E−05	3.900E−03	1.843E+01	5.165E−04
Tunnel width	18	2.964E+02	3.692E+03	6.077E+01	2.050E+01	1.432E+01
Septal spacing	12	1.860E+02	6.862E+02	2.620E+01	1.408E+01	7.562E+00
Half length/radius vector	46	1.815E+00	3.758E−02	1.939E−01	1.068E+01	2.858E−02
Radius vector	37	7.900E−01				
Half length	28	1.402E+00	1.751E−02	1.323E−01	9.438E+00	2.501E−02
Volution height	37	2.499E−01	3.181E−04	1.784E−02	7.136E+00	2.932E−03
Wall thickness	37	2.486E−02	1.084E−05	3.293E−03	1.324E+01	5.413E−04
Tunnel width	6	3.527E+02	2.803E+03	5.295E+01	1.501E+01	2.162E+01
Septal spacing	9	2.488E+02	1.937E+02	1.392E+01	5.594E+00	4.639E+00
Half length/radius vector	28	1.775E+00	2.806E−02	1.675E−01	9.438E+00	3.166E−02
Radius vector	7	1.000E+00				
Half length	6	1.742E+00	5.657E−03	7.521E−02	4.318E+00	3.070E−02
Volution height	7	2.973E−01	4.786E−04	2.188E−02	7.359E+00	8.268E−03
Wall thickness	7	2.786E−02	1.048E−05	3.237E−03	1.162E+01	1.223E−03
Half length/radius vector	6	1.742E+00	5.657E−03	7.521E−02	4.318E+00	3.070E−02

form ratio of *F. alaskensis* is consistently larger, the septal spacing is consistently wider, the tunnel is consistently narrower, and there is considerable overlap in wall thickness. Except for wall thickness, many of the *F. bocki* group are in intermediate positions between these two species. The wall in most of the other forms is thicker.

Material studied.—*F. alaskensis* n. sp. is common at localities 31 and 32 where it occurs in a number of samples (see locality descriptions) but is most common in samples f23977 and f23979 at locality 31 and sample f23986 at locality 32. Seventy-eight oriented sections were measured and many others studied in 171 thin sections.

F. alaskensis n. sp. occurs in association with textularids, *Tetrataxis* sp., endothyrids including *Bradyina* sp., *Ozawinella*?, and *Fusulina flexuosa* n. sp. In addition, in sample f23986 it is associated with *Beedeina*?

Designation of types.—The specimen illustrated on plate 4 as figure 6 and plate 5 as figure 1 is designated the holotype. The other specimens studied are paratypes.

Genus FUSULINA Fischer de Waldheim 1829

Fusulina flexuosa n. sp.

Plate 7, figures 1–20

Diagnosis.—Shell small, attaining lengths up to 9 mm and widths of 1.5 mm in 6 volutions. The shape is irregular subcylindrical, commonly with an irregular axis. The inner volutions are rather fusiform with relatively pointed poles. The coiling is relatively tight with numerous septa in each volution. Chomata are weakly developed. The spirotheca is thin and composed of tectum and diaphanotheca and locally developed tectoria.

Description.—Summaries of the numerical data are given in table 4. The spiral form is normal negative increasing regularly through all but the last volutions in which the rate of increase diminishes as shown in figure 8. The volution height increases with increasing radius as shown for the combined samples in figure 9.

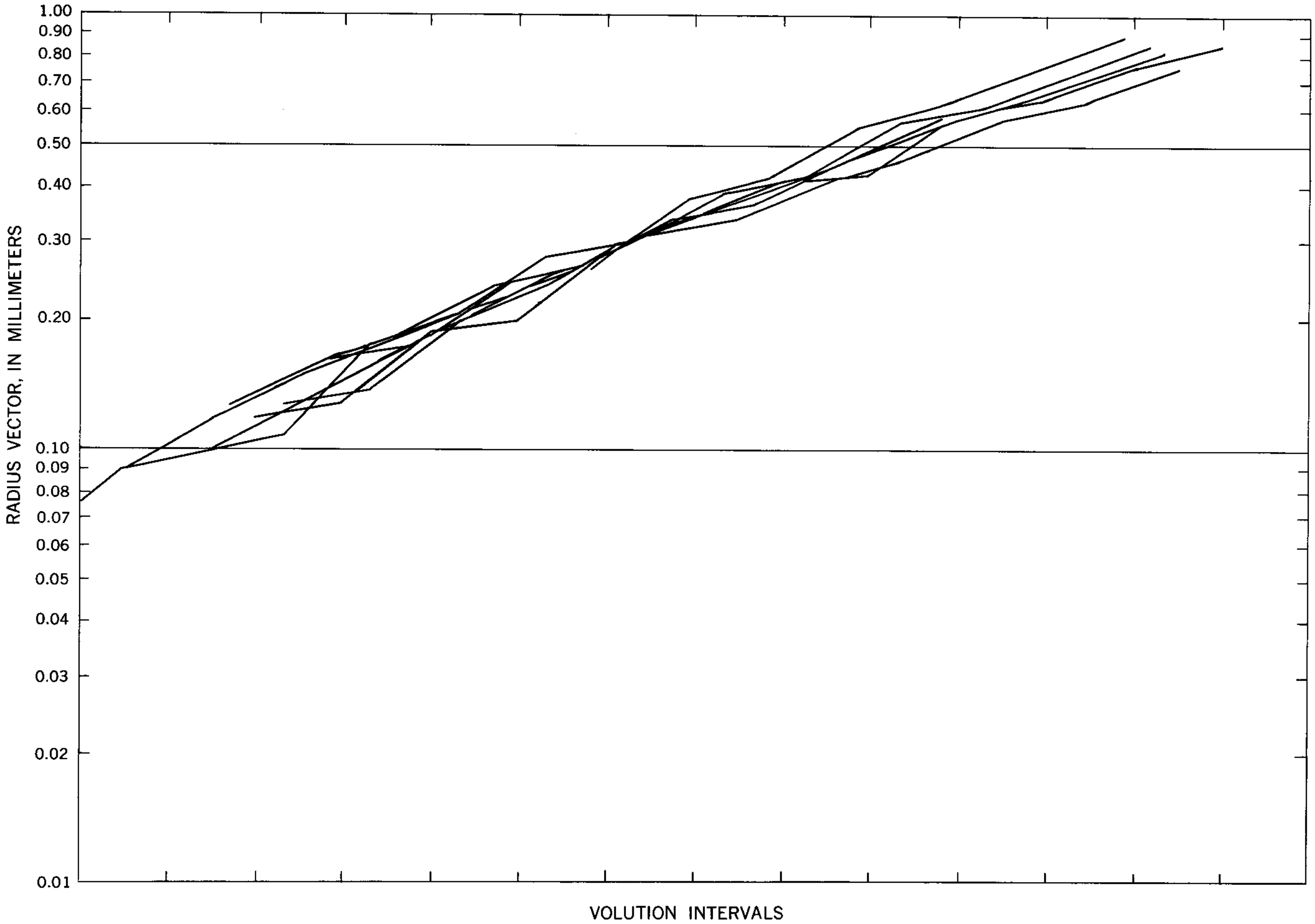

FIGURE 8.—The spiral form of *Fusulina flexuosa* n. sp. shown by a plot of radius vector on a logarithmic scale against volution intervals on an arithmetic scale. Six specimens from samples f23979, f23981, and f23986 are represented.

TABLE 4.—*Summary numerical data for* Fusulina flexuosa *n. sp.*

[The data are presented at standard radii. All numbers are expressed in exponential notation. The number of digits recorded does not imply degree of accuracy recorded]

Character	Number of specimens	Mean	Variance	Standard deviation	Coefficient of variability	Standard error of the mean
Radius vector	3	1.000E−01				
Half length	2	1.700E−01	2.000E−04	1.414E−02	8.319E+00	1.000E−02
Volution height	3	3.867E−02	5.333E−06	2.309E−03	5.973E+00	1.333E−03
Tunnel width	3	4.333E+01	3.333E+01	5.774E+00	1.332E+01	3.333E+00
Half length/radius vector	2	1.700E+00	2.000E−02	1.414E−01	8.319E+00	1.000E−01
Radius vector	9	1.300E−01				
Half length	8	2.212E−01	5.355E−03	7.318E−02	3.308E+01	2.587E−02
Volution height	8	5.050E−02	4.857E−05	6.969E−03	1.380E+01	2.464E−03
Wall thickness	7	9.143E−03	5.476E−06	2.340E−03	2.560E+01	8.845E−04
Tunnel width	6	7.417E+01	7.146E+02	2.673E+01	3.604E+01	1.091E+01
Half length/radius vector	8	1.702E+00	3.169E−01	5.629E−01	3.308E+01	1.990E−01
Radius vector	13	1.600E−01				
Half length	12	3.292E−01	2.481E−03	4.981E−02	1.513E+01	1.438E−02
Volution height	13	6.331E−02	1.377E−04	1.174E−02	1.854E+01	3.255E−03
Wall thickness	12	1.158E−02	2.083E−06	1.443E−03	1.246E+01	4.167E−04
Tunnel width	9	9.800E+01	6.358E+02	2.521E+01	2.573E+01	8.405E+00
Half length/radius vector	12	2.057E+00	9.692E−02	3.113E−01	1.513E+01	8.987E−02
Radius vector	17	2.000E−01				
Half length	16	4.781E−01	6.403E−03	8.002E−02	1.674E+01	2.000E−02
Volution height	17	7.147E−02	4.314E−05	6.568E−03	9.190E+00	1.593E−03
Wall thickness	16	1.300E−02	5.733E−06	2.394E−03	1.842E+01	5.986E−04
Tunnel width	14	1.367E+02	2.259E+03	4.753E+01	3.477E+01	1.270E+01
Half length/radius vector	16	2.391E+00	1.601E−01	4.001E−01	1.674E+01	1.000E−01
Radius vector	18	2.500E−01				
Half length	17	6.747E−01	9.389E−03	9.690E−02	1.436E+01	2.350E−02
Volution height	18	8.956E−02	1.147E−04	1.071E−02	1.196E+01	2.525E−03
Wall thickness	18	1.439E−02	4.840E−06	2.200E−03	1.529E+01	5.185E−04
Tunnel width	14	1.624E+02	2.412E+03	4.912E+01	3.024E+01	1.313E+01
Half length/radius vector	17	2.699E+00	1.502E−01	3.876E−01	1.436E+01	9.400E−02
Radius vector	18	3.200E−01				
Half length	17	9.159E−01	2.441E−02	1.562E−01	1.706E+01	3.790E−02
Volution height	18	1.065E−01	1.413E−04	1.189E−02	1.116E+01	2.802E−03
Wall thickness	18	1.678E−02	1.089E−05	3.300E−03	1.967E+01	7.778E−04
Tunnel width	12	2.229E+02	4.601E+03	6.783E+01	3.043E+01	1.958E+01
Half length/radius vector	17	2.862E+00	2.384E−01	4.883E−01	1.706E+01	1.184E−01
Radius vector	17	4.000E−01				
Half length	16	1.217E+00	4.015E−02	2.004E−01	1.646E+01	5.010E−02
Volution height	17	1.231E−01	2.072E−04	1.440E−02	1.169E+01	3.491E−03
Wall thickness	16	1.900E−02	9.333E−06	3.055E−03	1.608E+01	7.638E−04
Tunnel width	8	3.160E+02	7.585E+03	8.709E+01	2.756E+01	3.079E+01
Half length/radius vector	16	3.044E+00	2.510E−01	5.010E−01	1.646E+01	1.252E−01
Radius vector	15	5.000E−01				
Half length	15	1.619E+00	8.017E−02	2.831E−01	1.749E+01	7.311E−02
Volution height	15	1.477E−01	1.151E−04.	1.073E−02	7.261E+00	2.770E−03
Wall thickness	15	2.073E−02	1.278E−05	3.575E−03	1.724E+01	9.231E−04
Tunnel width	5	5.064E+02	2.986E+04	1.728E+02	3.412E+01	7.728E+01
Half length/radius vector	15	3.237E+00	3.207E−01	5.663E−01	1.749E+01	1.462E−01
Radius vector	9	6.300E−01				
Half length	9	2.169E+00	1.816E−01	4.261E−01	1.965E+01	1.420E−01
Volution height	9	1.867E−01	6.985E−04	2.643E−02	1.416E+01	8.810E−03
Wall thickness	9	2.222E−02	2.494E−05	4.994E−03	2.247E+01	1.665E−03
Half length/radius vector	9	3.443E+00	4.575E−01	6.764E−01	1.965E+01	2.255E−01
Radius vector	5	7.900E−01				
Half-length	5	2.964E+00	2.720E−01	5.216E−01	1.760E+01	2.333E−01
Volution height	5	2.140E−01	1.085E−04	1.042E−02	4.867E+00	4.658E−03
Wall thickness	4	2.325E−02	2.092E−05	4.573E−03	1.967E+01	2.287E−03
Half length/radius vector	5	3.752E+00	4.359E−01	6.602E−01	1.760E+01	2.953E−01

The shell length increases in relation to the width at a rate more rapid than simple logarithmic growth (fig. 9). This feature is reflected in the plot of form ratio against radius (fig. 9); the form ratio increases rapidly in the earlier stages of growth and increases less rapidly to maturity. The axis of coiling varies from nearly straight to highly irregular, commonly curved in more than one plane.

The proloculus ranges from 120 to 340 microns in diameter (fig. 9), although most specimens fall in the 150 to 280 micron range. The larger proloculi are of irregular shape. No microspheric specimens were recognized.

The wall thickness increases regularly through the smaller parts of the test and then less rapidly in the last stages of growth (fig. 9). The wall is composed of a thin tectum and a diaphanotheca. Inner and outer tectoria are developed intermittently but are never prominent.

The septa are irregular but tend to be tightly fluted across the entire length of the test They are less fluted in the inner volutions, especially in the forms with smaller proloculi (pl. 7, figs. 2a, b). The septa appear closely spaced, but not enough spacing data are available for a meaningful statement.

The tunnel is poorly defined, wanders in the equatori-

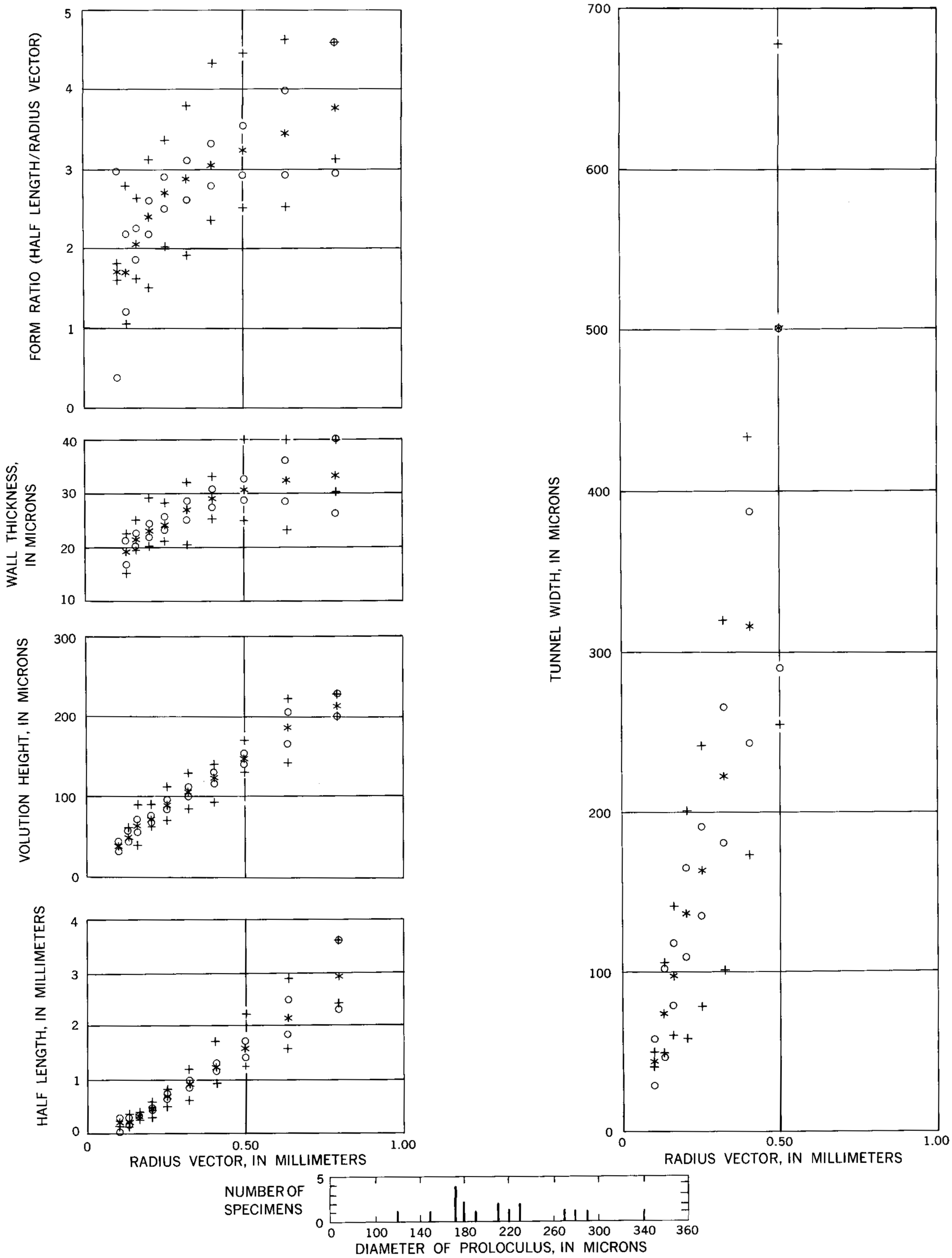

Figure 9.—Summary graphs for *Fusulina flexuosa* n. sp. The half length, volution height, wall thickness, form ratio, and tunn width are each plotted against the radius vector. This shows the changes for each character during the ontogeny. Tl mean(*), confidence limits on the mean(o–o), and maximum and minimum (+–+) are shown at each standard radius. Tl numerical values for the means and confidence limits and the number of specimens on which each is based are given table 4. The diameters of proloculi are plotted against the number of specimens.

al plane, and is bordered by low, discontinuous chomata or parachomata. The tunnel height varies from less than half to possibly the entire height of the chamber. The tunnel width increases rapidly (fig. 9), but measurements in the outer volutions are probably not reliable because of indeterminate tunnel margins.

Axial filling is present, especially in the inner volutions, but it is irregular and does not appear in all specimens.

Comparison and remarks.—*Fusulina flexuosa* n. sp. is related to a general group that includes the type species, *F. cylindrica* Fischer de Waldheim 1829, *F. ? occasa* Thompson 1965, and *Akiyoshiella toriyamai* Thompson, Pitrat, and Sanderson 1953. A meaningful comparison with these forms is difficult because little data are available for them. The range of variability of *Fusulina flexuosa* n. sp. is sufficient to overlap that of the three forms above, but without additional data on the latter their variability cannot be determined. It is possible that each named form, when properly studied, will show more limited ranges within the general areas of overlap; therefore they are not being combined at this time.

Material studied.—*F. flexuosa* n. sp. was recognized in samples f23977 and f23981 of locality 31 and in sample f23986 at locality 32. Eighteen oriented thin sections were measured and many others studied in about 50 thin sections. *F. flexuosa* n. sp. occurs with *Tetrataxis* sp., endothyrids, *Ozawainella?*, *Fusulinella alaskensis*, and (in sample f23986) *Beedeina?*

Designation of types.—The specimen illustrated on plate 7 as figures 1a–b is designated the holotype. The other specimens studied are paratypes.

Genus BEEDEINA Galloway 1933

Beedeina? sp.

Plate 6, figures 16, 17a–b

The genus *Beedeina* as discussed by Ishii (1957, p. 655) and others seems to be represented in the Alaskan collections by a relatively small, tightly coiled form resembling *Fusulina ylychensis* Rauser 1951 (in Rauser-Chernoussova and others, 1951, p. 296). Only two oriented sections were obtained. These show the tight coiling, closely spaced and tightly fluted septa, moderately thick wall composed of tectum, diaphanotheca, and tectoria, a relatively narrow tunnel well defined by asymmetrical chomata, and no other obvious epithecal deposits. These specimens cannot be assigned to *Fusulinella alaskenis* n. sp. or to *Fusulina flexuosa* n. sp., the other larger fusulinids found in this sample. They are not typical of *Beedeina* either, but seem to be within the morphologic range of that genus.

REFERENCES CITED

Douglass, R. C., 1970, Morphologic studies of fusulinids from the Lower Permian of West Pakistan: U.S. Geol. Survey Prof. Paper 643–G, 13 p., 7 pls., 6 text figs.

Dunbar, C. O., and Newell, N. D., 1946, Marine Early Permian of the Central Andes and its fusuline faunas: Am. Jour. Sci., v. 244, no. 6, p. 377–402; no. 7, p. 457–491, pls. 1–12.

Dutkevich, G, A., 1934, Some new species of Fusulinidae from the Upper and Middle Carboniferous of Verkhne-Chussovskye Gorodki of the Chussovaya River (western slope of the middle Urals): [U.S.S.R.] Neftyanoi Geologo-Rezvedochnyi Inst. Trudy, ser. A, v. 36, p. 1–98, pls. 1–6. [In Russian, English summary.]

Dutro, J. T., Jr., and Douglass, R. C., 1961, Pennsylvanian rocks in southeastern Alaska, *in* Geological Survey research 1961: U.S. Geol. Survey Prof. Paper 424–B, p. B239–B241, 1 text fig.

Ehrenberg, C. G., 1854, Mikrogeologie: Leipzig, L. Voss, 374 p., 40 pls.

Fischer de Waldheim, G., 1829, Sur les Cephalopodes fossiles de Moscou et de ses environs, en montrant des objects en nature: Moscuo Imp. Soc. Nat. Bull., v. 1, p. 300–331.

Forbes, C. L., 1960, Carboniferous and Permian Fusulinidae from Spitsbergen: Palaeontology, v. 2, pt. 2, p. 210–225, pls. 30–33, 1 fig., 1 table.

Galloway, J. J., 1933, A manual of Foraminifera (James Furman Kemp memorial series Pub. no. 1): Bloomington, Ind., The Principia Press Inc., 483 p., 42 pls.

Ginkel, A. C. van, 1965, Carboniferous fusulinids from the Cantabrian Mountains (Spain): Leidse Geol. Meded., v. 34, p. 1–225, pls. 1–53, 13 figs, maps, correlation charts.

Igo, Hisayoshi, 1957, Fusulinids of Fukuji, southeastern part of the Hida Massif, Central Japan: Tokyo Kyoiku Daigaku Sci. Repts., sec. C, no. 47, p. 153–246, pls. 1–15, 2 text figs.

Ishii, Ken-ichi, 1957, On the so-called *Fusulina*: Japan Acad. Proc. v. 33, no. 10, p. 652–656, 2 text-figs.

——— 1958a, Fusulinids from the middle Upper Carboniferous Itadorigawa group in western Shikoku, Japan; part I Genus *Fusulina*: Osaka City Univ., Inst. Polytech. Jour., ser. G, Geoscience, v. 4, p. 1–28, pls. 1–5, tables 1–3.

——— 1958b, On the phylogeny, morphology and distribution of *Fusulina*, *Beedeina* and allied fusulind genera: Osaka City Univ., Inst. Polytech. Jour., ser. G, Geoscience, v. 4, p. 29–70, pls. 1–4, text figs. 1–5

——— 1962, Fusulinids from the middle Upper Carboniferous Itadorigawa Group in western Shikoku, Japan Part II. Genus *Fusulinella* and other fusulinids: Osaka City Univ. Jour. Geosciences, v. 6, art. 1, p. 1–43, pls. 6–12.

Lee, J. S., 1933, Taxonomic criteria of Fusulinidae with notes on seven new Permian genera: Natl. Research Inst. of Geology (Acad. Sinica), Mem., v. 14, p. 1–32, pls. 1–5, 8 text figs.

Möller, V. von, 1878, Die Spiral-Gewundene Forminiferen des Russischen Kohlen Kalks: St. Petersbourg Akad. Imp. Sci. Mem., ser. 7, v. 25, no. 7, p. 1–147, pls. 1–15.

——— 1879, Die Foraminiferen des russischen Kohlen Kalks: St. Petersbourg Akad. Imp. Sci. Mem., ser 7, v. 27, p. 1–131, pls. 1–7, text figs 1–30.

Muffler, L. J. P., 1967, Stratigraphy of the Keku Islets and neighboring parts of Kuiu and Kupreanof Islands, southeastern Alaska: U.S. Geol. Survey Bull. 1241–C, p. 1–52, pl. 1, figs. 1–15.

Ozawa, Yoshiaki, 1925, On the classification of Fusulinidae: Tokyo Imp. Univ. Jour. Coll. Sci., v. 45, art. 4, p. 1–26, pls. 1–4, 3 text figs.

Rauser-Chernoussova D. M., and others, 1951, Middle Carboniferous fusulinids of the Russian Platform and adjoining regions: Moscow, Akad. Nauk SSSR, Inst. Geol. Nauk, 380 p., 58 pls., 30 text figs. (in Russian).

Simpson, G. G., Roe, Anne, and Lewontin, R. C., in 1960, Quantitative zoology, revised ed.: New York, Harcourt, Brace and Company, 440 p., 64 figs.

Skinner, J. W. and Wilde, G. L., 1954, New early Pennsylvanian fusulinids from Texas: Jour. Paleontology, v. 28, no. 6, p. 796–803, pls. 95–96.

Thompson, M. L., 1935, The fusulinid genus *Staffella* in America: Jour. Paleontology, v. 9, no. 2, 111–120, pl. 13.

——— 1942, New genera of Pennsylvanian fusulinids: Am. Jour. Sci., v. 240, p. 403–420, pls. 1–3.

——— 1947. Stratigraphy and fusulinids of pre-Desmoinesian Pennsylvanian rocks, Llano Uplift, Texas: Jour. Paleontology, v. 21, no. 2, p. 147–164, pls. 31–33, 2 text figs.

——— 1948, Protozoa; Studies of American fusulinids: Kansas Univ. Paleont. Contr., art. 1, p. 1–184, pls. 1–38, 7 text figs.

——— 1965, Pennsylvanian and Early Permian fusulinids from Fort St. James area, British Columbia, Canada: Jour. Paleontology, v. 39, no. 2, p. 224–234, pls. 33–35, 1 text fig.

Thompson, M. L., Pitrat, C. W., and Sanderson, G. A., 1953, Primitive Cache Creek fusulinids from central British Columbia: Jour. Paleontology, v. 27, no. 4, p. 545–552, pls. 57–58.

Toriyama, Ryuzo, 1953, New peculiar fusulinid genus from the Akiyoshi limestone of southwestern Japan: Jour. Paleontology, v. 27, p. 251–256, pls. 35, 36, tables 1, 2.

——— 1958, Geology of Akiyoshi; part 3, Fusulinids of Akiyoshi: Kyushu Univ., Fac. Sci. Mem., ser. D, v. 7, 264 p., 48 pls.

INDEX

[Italic page numbers indicate major references and descriptions]

U. S. GOVERNMENT PRINTING OFFICE : 1971 O - 419-577

PLATES 1–7

[Contact photographs of the plates in this report are available, at cost, from U.S. Geological Survey Library, Federal Center, Denver, Colorado 80225]

PLATE 1

FIGURES 1–3. *Tetrataxis* sp. (p. 4) from locality 29 Ladrones Islands.

1a–b. Axial section × 10 and × 50, specimen f23973–28, USNM 167022.

2a–b. Axial section × 10 and × 50, specimen f23973–31, USNM 167023.

3. Axial section × 50, specimen f23974–1, USNM 167024.

4, 5. Endothyrid undet. (p. 5) from locality 29 Ladrones Islands.

4. Axial section × 50, specimen f23974–12, USNM 167025.

5. Axial section × 50, specimen f23974–3, USNM 167026.

6–22. *Nankinella* sp. (p. 5) from locality 29 Ladrones Islands.

6a–b. Axial section × 10 and × 50, specimen f23973–16, USNM 167027.

7a–b. Axial section × 10 and × 50, specimen f23973–3, USNM 167028.

8a–b. Equatorial section × 10 and × 50, specimen f23974–20, USNM 167029.

9a–b. Equatorial section × 10 and × 50, specimen f23974–4, USNM 167030.

10. Axial section × 50, specimen f23974–17, USNM 167031.

11. Axial section × 50, specimen f23973–2, USNM 167032.

12. Axial section × 50, specimen f23973–39, USNM 167033.

13. Axial section × 50, specimen f23973–35, USNM 167034.

14. Equatorial section × 50, specimen f23973–33, USNM 167035.

15. Subaxial section × 50, specimen f23973–28, USNM 167036.

16. Axial section × 50, specimen f23973–33, USNM 167037.

17. Deep tangential section × 50, specimen f23974–3, USNM 167038.

18. Subaxial section × 50, specimen f23974–9, USNM 167039.

19. Subaxial section × 50, specimen f23974–5, USNM 167040.

20. Axial section with twisted axis × 50, specimen f23973–35, USNM 167041.

21. Tangential section × 50, specimen f23974–8, USNM 167042.

22. Tangential section × 50, specimen f23973–17, USNM 167043.

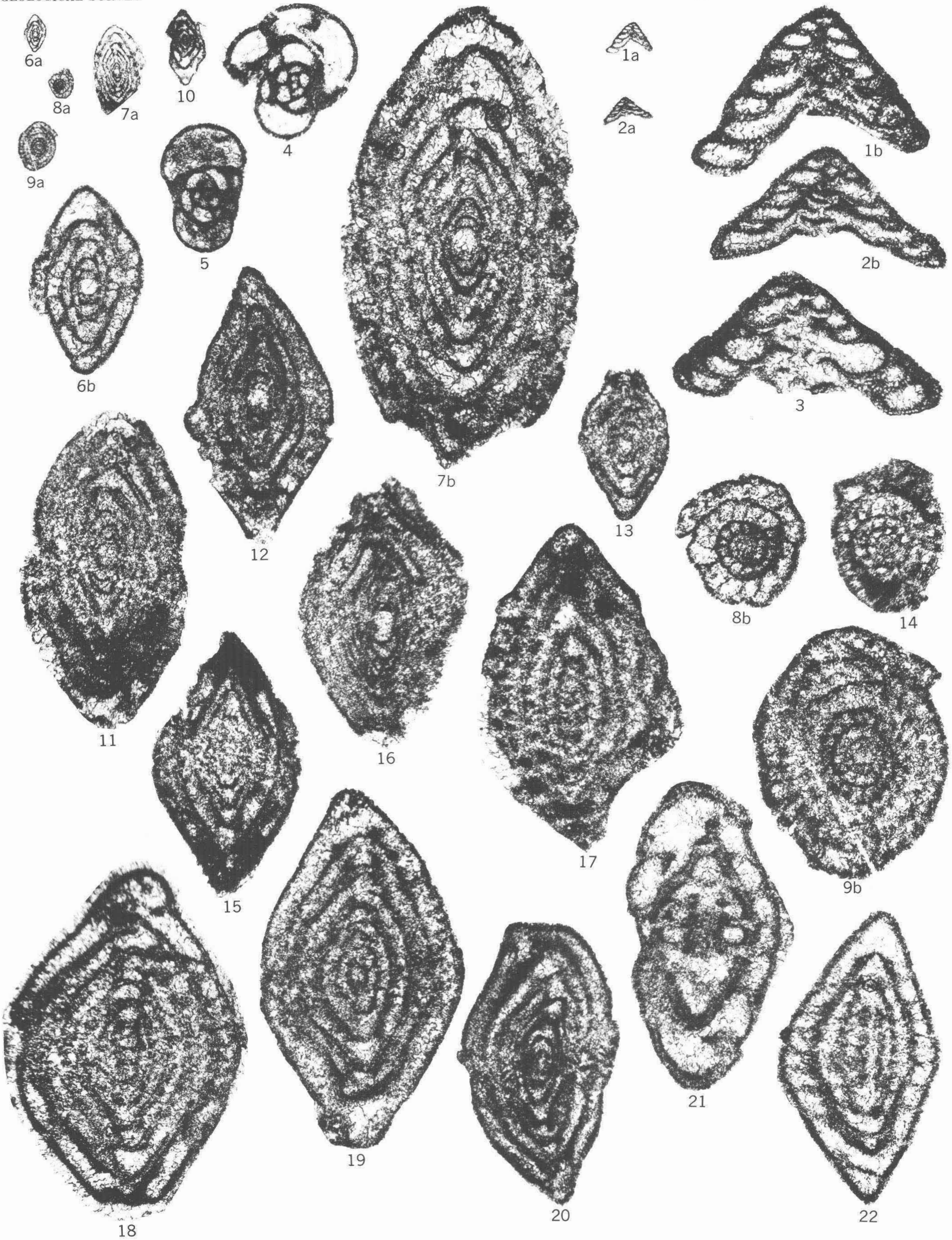

TETRATAXIS, ENDOTHYRIDS, AND *NANKINELLA* SP.
FROM LADRONES ISLANDS

PLATE 2

FIGURE 1. *Staffella* sp. aff. *S. powwowensis* Thompson 1948 (p. 5) from locality 30 on Peratovich Island. Axial section × 50, specimen f23975–13, USNM 167044.

2–3. *Millerella* sp. aff *M. marblensis* Thompson 1942, (p. 5) from locality 30 on Peratovich Island.

2. Axial section × 50, specimen f23975–4, USNM 167045.
3. Axial section × 50, specimen f23975–8, USNM 167046.

4–21. *Pseudostaffella rotunda* Dougiass, n. sp. (p. 6) from locality 30 on Peratovich Island.

4a–b. Axial section of the holotype × 10 and × 50, specimen f23975–12, USNM 167047.
5a–b. Oblique deep tangential section × 10 and ×50 showing the relationship between the chomata and the septa, specimen f23976–1, USNM 167048
6a–b. Axial section × 10 and × 50, specimen f23975–8, USNM 167049.
7. Equatorial section × 10, specimen f23975–6, USNM 167050.
8a–b. Equatorial section × 10 and × 50, specimen f23975–5, USNM 167051.
9a–b. Equatorial section × 10 and × 50, specimen f23975–4, USNM 167052.
10a–b. Oblique equatorial section × 10 and × 50, specimen f23975–3, USNM 167053.
11a–b. Equatorial section × 10 and × 50, specimen f23976–2, USNM 167054.
12. Tangential section × 50, specimen f23975–11, USNM 167055.
13. Equatorial section × 50, specimen f23975–10, USNM 167056.
14. Equatorial section × 50, specimen f23976–9, USNM 167057.
15. Axial section × 50, specimen f23976–4, USNM 167058.
16. Axial section × 50, specimen f23975–11, USNM 167059.
17. Axial section × 50, specimen f23976–5, USNM 167060.
18. Equatorial section × 50, specimen f23976–6, USNM 167061.
19. Equatorial section × 50, specimen f23975–7, USNM 167062.
20. Equatorial section × 50, specimen f23975–9, USNM 167063.
21. Equatorial section × 50, specimen f23976–7, USNM 167064.

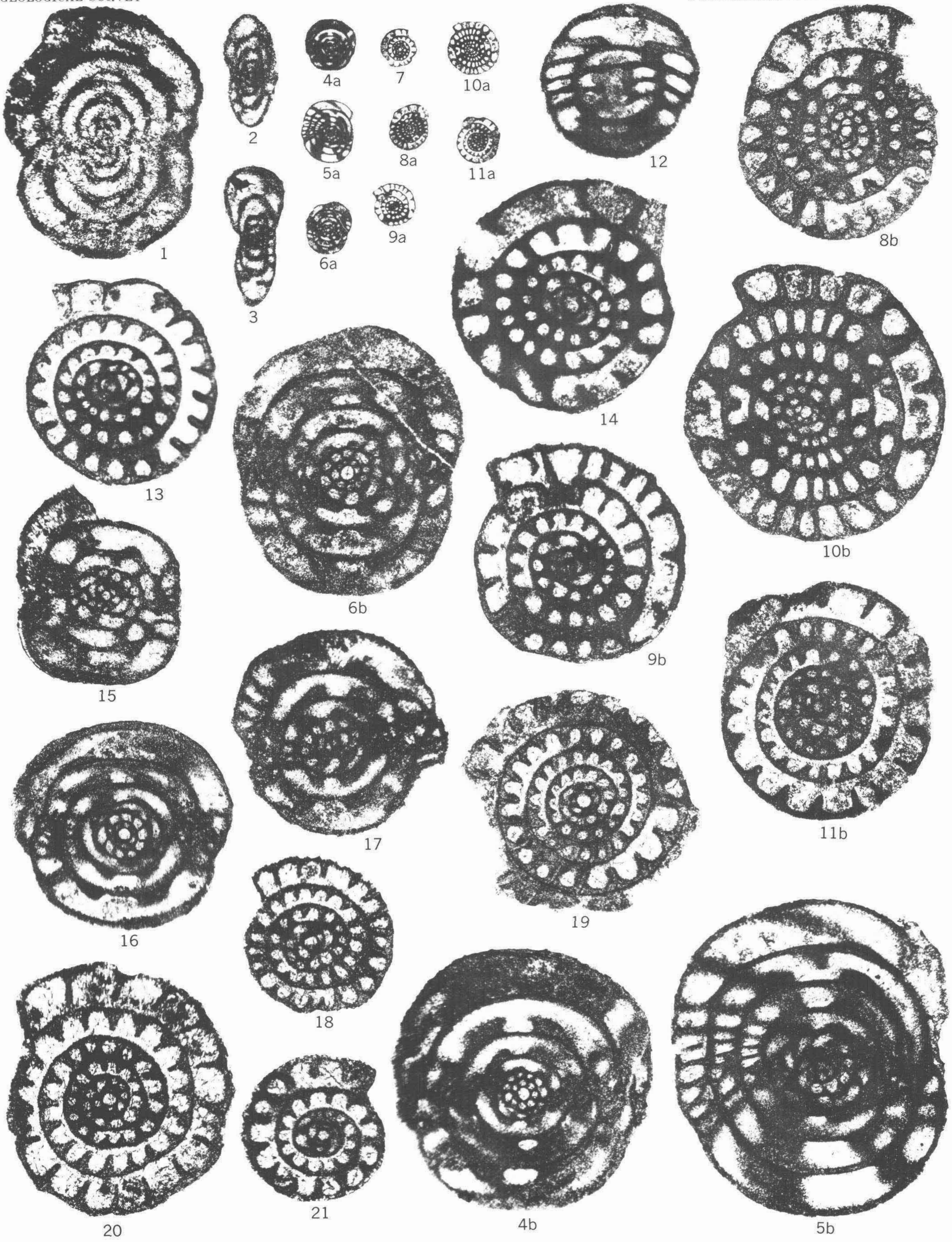

STAFFELLA, MILLERELLA, AND *PSEUDOSTAFFELLA ROTUNDA* DOUGLASS, N. SP., FROM PERATROVICH ISLAND

PLATE 3

FIGURES 1–28. *Fusulinella pinguis* Douglass, n. sp. (p. 9) from locality 29, Ladrones Islands.

1a–b. Axial section of the holotype × 10 and × 50, specimen f23973–3, USNM 167065.
2. Axial section × 10, specimen f23973–5, USNM 167066.
3. Axial section × 10, specimen f23973–12, USNM 167067.
4. Axial section × 10, specimen f23973–14, USNM 167068.
5. Axial section × 10, specimen f23973–22, USNM 167069.
6a–b. Axial section × 10 and × 50, specimen f23973–24, USNM 167070. A microspheric specimen.
7. Axial section × 10, specimen f23974–5, USNM 167071.
8. Axial section × 10, specimen f23974–12, USNM 167072.
9. Axial section × 10, specimen f23974–15, USNM 167073.
10. Axial section × 10, specimen f23974–1, USNM 167074.
11. Axial section × 10, specimen f23974–3, USNM 167075.
12. Axial section × 10, specimen f23974–6, USNM 167076.
13. Equatoiial section × 10, specimen f23973–25, USNM 167077.
14. Equatorial section × 10, specimen f23973–27, USNM 167078.
15a–b. Equatorial section × 10 and × 50, specimen f23973–32, USNM 167079.
16. Equatorial section × 10, specimen f23973–37, USNM 167080.
17a–b. Equatorial section × 10 and × 50, specimen f23973–39, USNM 167081.
18. Tangential section × 10, specimen f23973–27, USNM 167082.
19. Tangenital section × 10, specimen f23974–22, USNM 167083.
20. Equatorial section × 10, specimen f23974–17, USNM 167084.
21. Equatorial section × 10, specimen f23974–22, USNM 167085.
22a–b. Equatorial section × 10 and × 50, specimen f23974–21, USNM 167086.
23. Equatorial section × 10, specimen f23974–16, USNM 167087.
24. Equatorial section × 10, specimen f23973–38, USNM 167088.
25. Rock slice × 10 showing axial, tangential and subequatorial section of *Fusulinella* and a subaxial section of *Nankinella*, slide f23974–9.
26. Rock slice × 10 showing random slices of *Fusulinella, Nankinella*, and a textularid, slide f23974–25, USNM 167089.
27. Axial section × 50, specimen f23974–8, USNM 167090.
28. Axial section × 50 from slice shown in fig. 25, specimen f23974–9, USNM 167091.

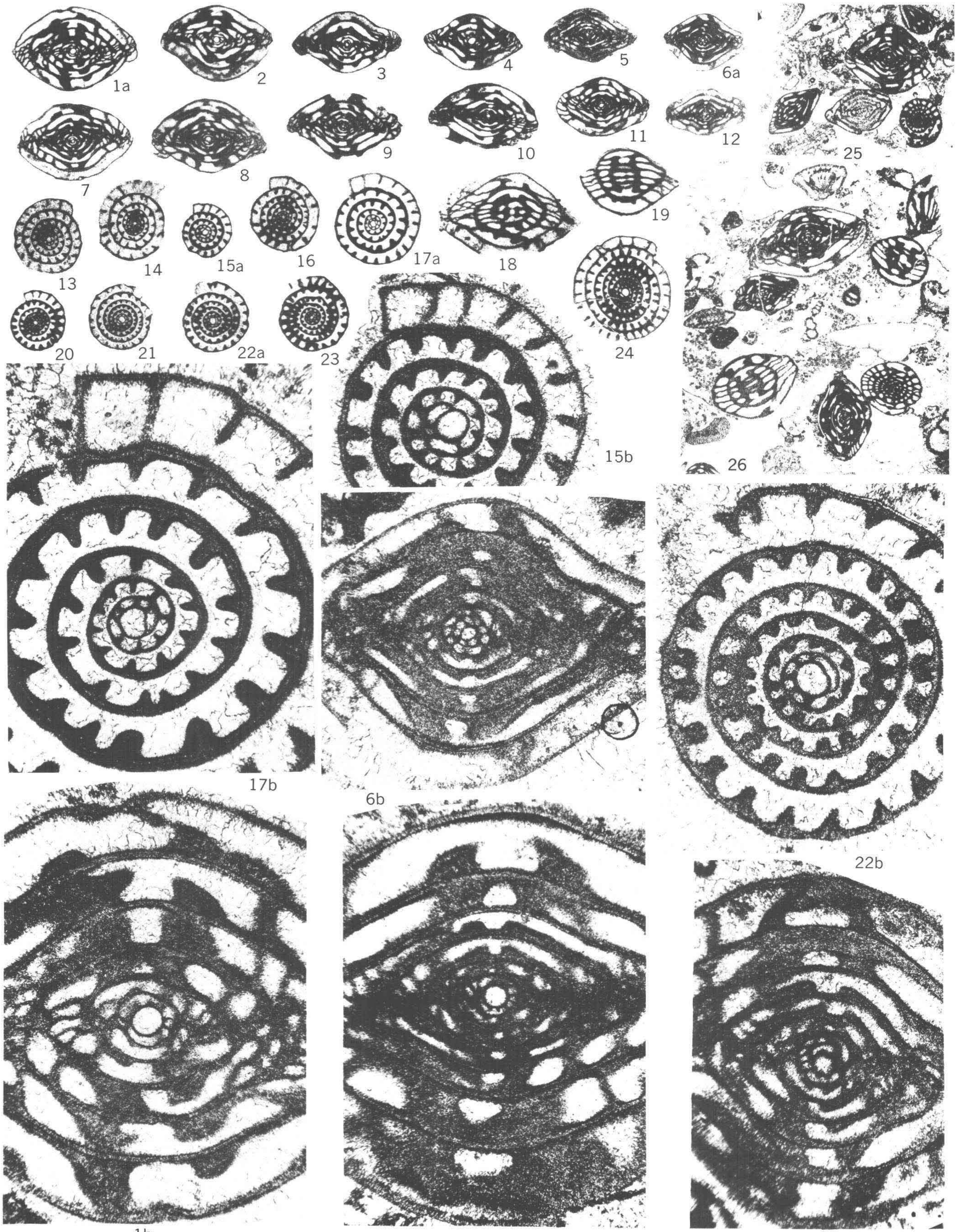

FUSULINELLA PINGUIS DOUGLASS, N. SP., FROM LADRONES ISLANDS

PLATE 4

FIGURE 1. *Bradyina* sp. (p. 5) from locality 31, Klawak inlet. Axial section × 10, specimen f23979–3, USNM 167092.

2–3. *Ozawainella?* sp. (p. 5) from locality 31, Llawak Inlet.

2. Tangential section × 50, specimen f23977–2, USNM 167093.
3. Oblique axial section × 50, specimen f23978–2, USNM 167094.

4–30. *Fusulinella alaskensis* Douglass, n. sp. (p. 12) from locality 31, Klawak Inlet.

4. Axial section × 10, specimen f23982–2, USNM 167095.

5a–b. Equatorial section × 10 and × 50, specimen f23982–4, USNM 167096.

6. Axial section of the holotype × 10, specimen f23982–1, USNM 167097.
7. Subaxial section × 10, specimen f23981–3, USNM 167098.
8. Equatorial section × 10, specimen f23980–5, USNM 167099.
9. Axial section × 10, specimen f23981–1 USNM 167100.
10. Axial section × 10, specimen f23980–2, USNM 167101.
11. Axial section × 10, specimen f23980–1, USNM 167102.
12. Axial section × 10, specimen f23979–5, USNM–167103.
13. Axial section × 10, specimen f23979–3 USNM 167104.
14. Axial section × 10, specimen f23979–2 USNM 167105.
15. Equatorial section × 10, specimen f23979–19, USNM 167106.
16. Equatorial section × 10, specimen f23979–16, USNM 167107.
17. Tangential section × 10, specimen f23979–19, USNM 167108.
18. Equatorial section × 10, specimen f23979–14, USNM 167109.
19. Equatorial section × 10, specimen f23979–20, USNM 167110.
20. Axial section × 10, specimen f23979–1, USNM 167111.
21. Axial section × 10, specimen f23979–8, USNM 167112.
22. Equatorial section × 10, f23977–12, USNM 167113.
23. Equatorial section × 10, specimen f23977–13, USNM 167114.

24a–b. Equatorial section × 10 and × 50, specimen f23977–14, USNM 167115.

25a–b. Equatorial section × 10 and × 50, specimen f23977–15, USNM 167116.

26. Axial section × 10, specimen f23977–11, USNM 167117.
27. Axial section × 10, specimen f23977–5, USNM 167118.
28. Axial section × 10, specimen f23977–8, USNM 167119.
29. Axial section × 10, specimen f23977–10, USNM 167120.
30. Juvenarium of microspheric specimen × 50, f23977–6, USNM 167121.

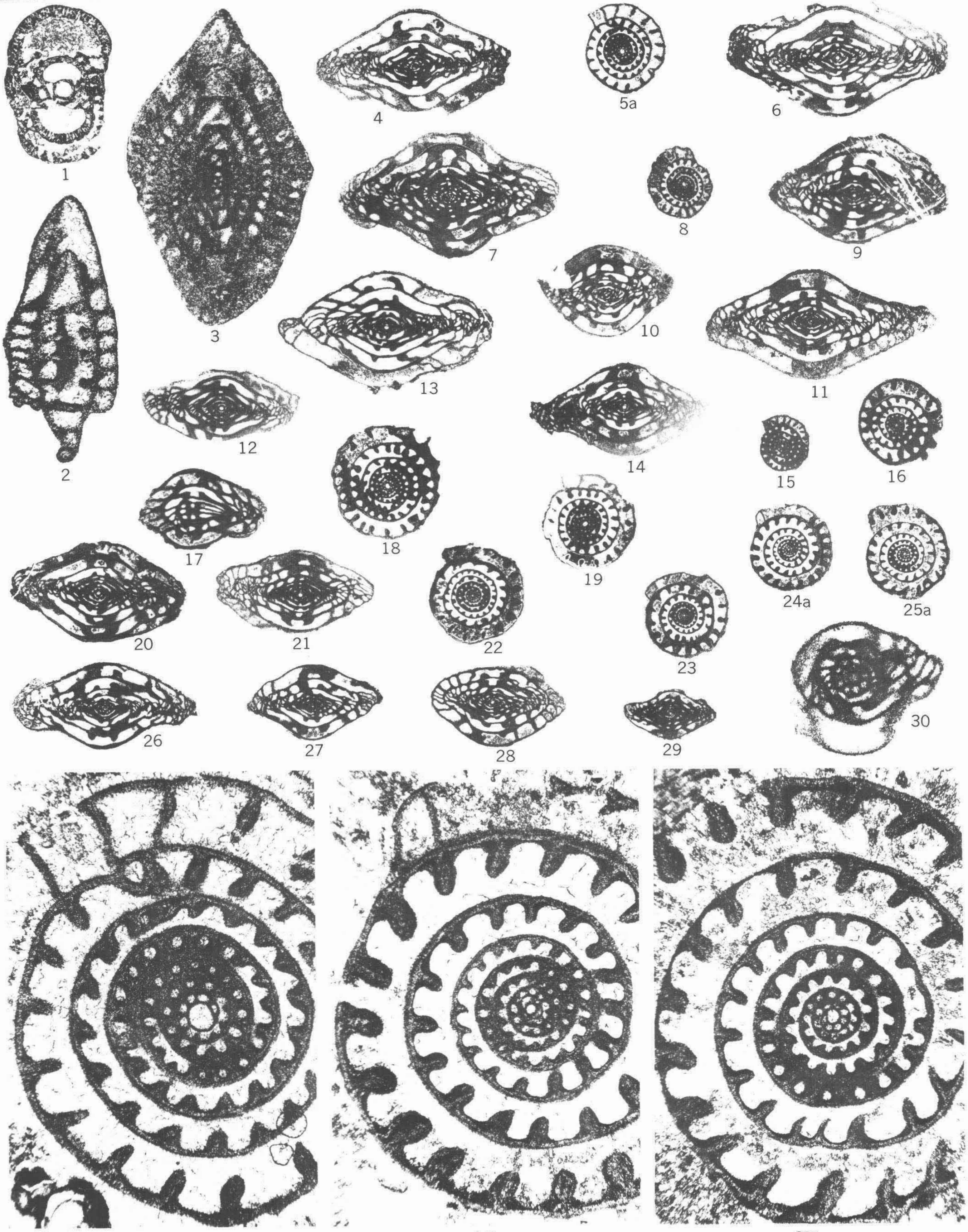

BRADYINA SP., *OZAWAINELLA*?, AND *FUSULINELLA ALASKENSIS* DOUGLASS, N. SP., FROM KLAWAK INLET

PLATE 5

FIGURES 1–8. *Fusulinella alaskensis* Douglass, n. sp. (p. 12) from locality 31, Klawak Inlet. All × 50.

1. Axial section of the holotype shown on pl. 4, fig. 6, showing the difference in appearance of the chomata at the septa and between septa. USNM 167097.
2. Subaxial section of the specimen shown on pl. 4 as fig. 7. The septa are in the plane of the section at the right side of the tunnel. Contrast this with the open look of fig. 5. USNM 167098.
3. Axial section of the specimen shown on pl. 4, fig. 11. The juvenariaum is at an angle to the adult and the proloculus is small, but the specimen is not a typical microspheric form. USNM 167102.
4. Axial section of a small specimen showing regular growth. Specimen f23979–11, USNM 167122.
5. Axial section of the specimen shown on pl. 4, fig. 13, showing the openness in most volutions where the septa are not intercepted. Note the chomata are formed in several layers of different densities. USNM 167104.
6. Subaxial section of a specimen that appears to have massive chomata because of the intersection of the septa in the plane of section. Specimen f23979–24, USNM 167123.
7. Axial section of the specimen shown on pl. 4, fig. 27, showing regular development from a relatively small proloculus, USNM 167118.
8. Axial section of the specimen shown on pl. 4, fig. 26 showing an endothyrid juvenarium with one volution at a large angle to the axis of the adult, USNM 167117.

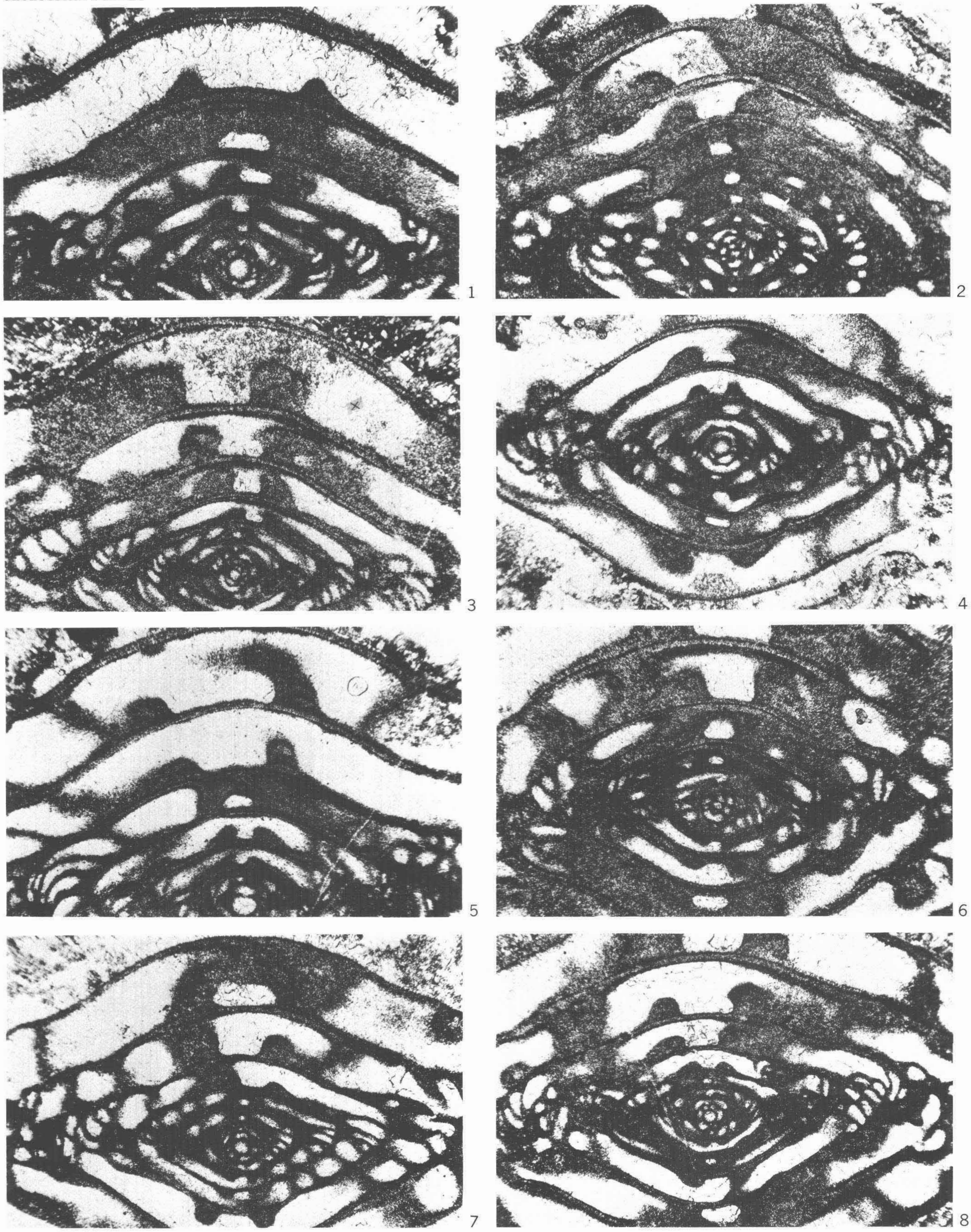

FUSULINELLA ALASKENSIS DOUGLASS, N. SP., FROM KLAWAK INLET

PLATE 6

FIGURES 1–15. *Fusilinella alaskensis* Douglass n. sp. (p. 12) from locality 32, sample f23986, Prince of Wales Island.

1. Axial section × 10, specimen 1, USNM 167124.

2a–b. Axial section × 10 and × 50, specimen 9, USNM 167125. Plane of septa nearly coincide with section in upper part giving the impression of more massive chomata.

3. Axial section × 10, specimen 10, USNM 167126.

4a–b. Axial section × 10 and × 50, specimen 16, USNM 167127.

5a–b. Equatorial section × 10 and × 50, specimen 42, USNM 167128.

6. Axial section × 10, specimen 20, USNM 167129.

7a–b. Axial section × 10 and × 50, specimen 2, USNM 167130 cut in a plane where many of the septa nearly coincide with the section and the impression of massive chomata is developed.

8. Axial section × 10, specimen 13, USNM 167131.

9. Axial section × 10, specimen 19, USNM 167132.

10. Axial section × 10, specimen 6, USNM 167133.

11. Tangential section × 10, specimen 29, USNM 167134.

12. Axial section × 10, specimen 23, USNM 167135.

13. Axial section × 10, specimen 12, USNM 167136.

14. Tangenital section × 10, from same thin section as specimen 2, figures 7a–b.

15. Axial section × 50, specimen 3, USNM 167137.

16–17. *Beedeina?* sp. (p. 19) from locality 32, sample f23986, Prince of Wales Island.

16. Equatorial section × 10, specimen 44, USNM 167138.

17a–b. Axial section × 10 and × 50, specimen 48, USNM 167139.

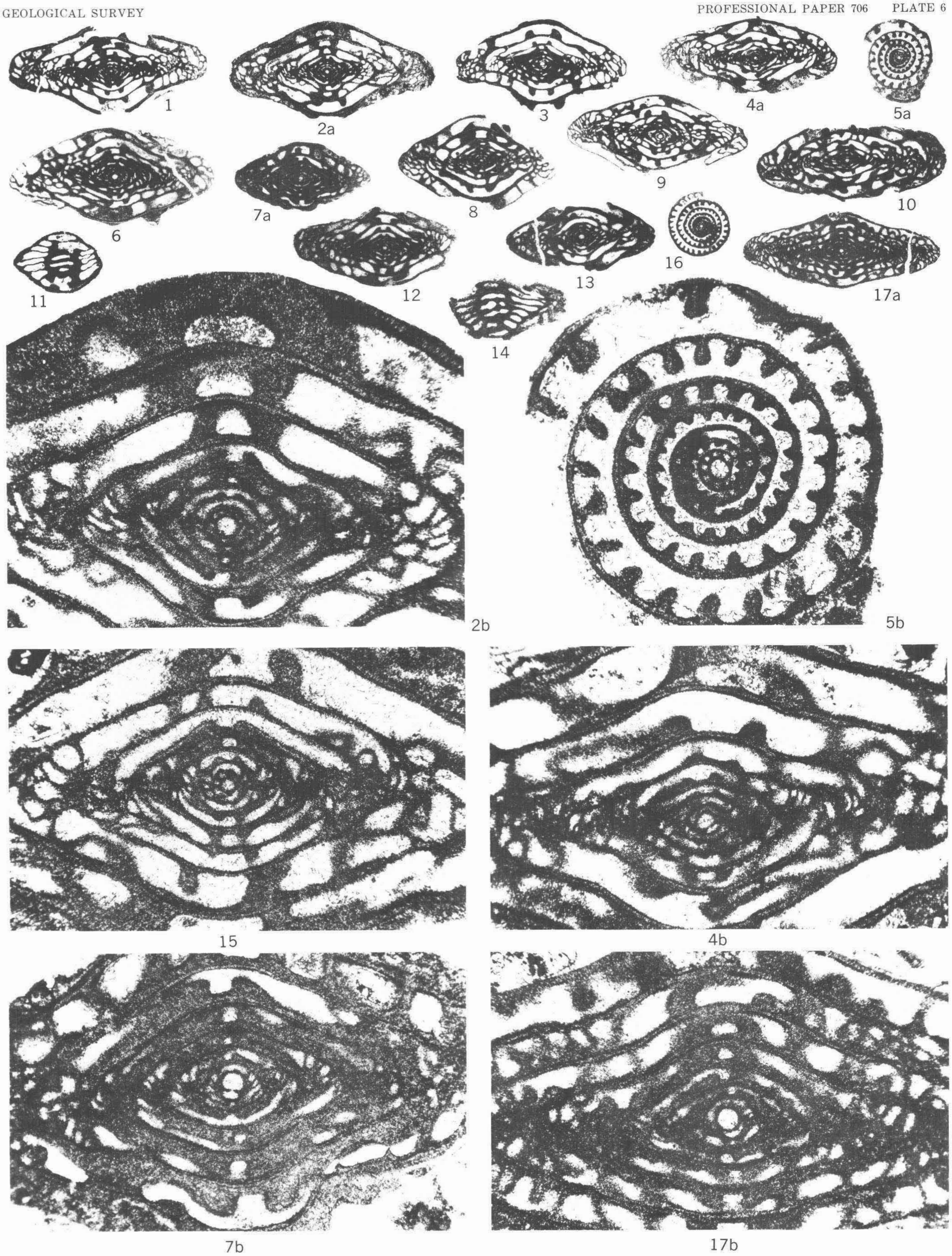

FUSULINELLA ALASKENSIS DOUGLASS, N.SP., AND *BEEDEINA*? SP.
FROM PRINCE OF WALES ISLAND

PLATE 7

FIGURES 1–20. *Fusulina flexuosa* Douglass, n. sp. (p. 16) from localities 31 and 32., Klawak Inlet and Prince of Wales Island.

1a–b. Axial section ×10 and ×50 of the holotype, one of the most regular specimens cut in a plane that misses most septa. Specimen f23977–17, USNM 167140.

2a–b. Axial section × 10 and × 50 of a specimen with small proloculus showing tightly coiled inner volutions. Specimen f23979–22, USNM 167141.

3a–b. Deep tangential section of a specimen with small proloculus showing discontinuous chomata even in the early volutions. Specimen f23986–36, USNM 167142.

4. Axial section × 10, partly silicified specimen f23979–21, USNM 167143.
5. Axial section × 10, specimen f23977–18, USNM 167144.
6. Deep tangential × 10, specimen f23979–23, USNM 167145.
7. Axial section × 10, specimen f23986–33, USNM 167146.
8. Axial section × 10, specimen f23981–8, USNM 167147.

9a–b. Axial section × 10 and × 50, specimen f23981–6, USNM 167148.

10a–b. Axial section × 10 and × 50, specimen f23986–28, USNM 167149.

11a–b. Axial section × 10 and × 50, specimen f23981–9, USNM 167150.

12. Axial section × 10, specimen f23981–7, USNM 167151.
13. Axial section × 10 of a specimen with a large proloculus. Specimen f23986–31, USNM 167152.
14. Axial section × 10, specimen f23986–29, USNM 167153.
15. Axial section × 10, specimen f23986–27, USNM 167154.
16. Axial section × 10, specimen f23986–30, USNM 167155.
17. Axial section × 10, specimen f23986–34, USNM 167156.
18. Subaxial section × 10, specimen f23986–35, USNM 167157.
19. Equatorial section × 10, specimen f23986–40, USNM 167158.
20. Tangential section × 10, specimen f23986–38, USNM 167159.

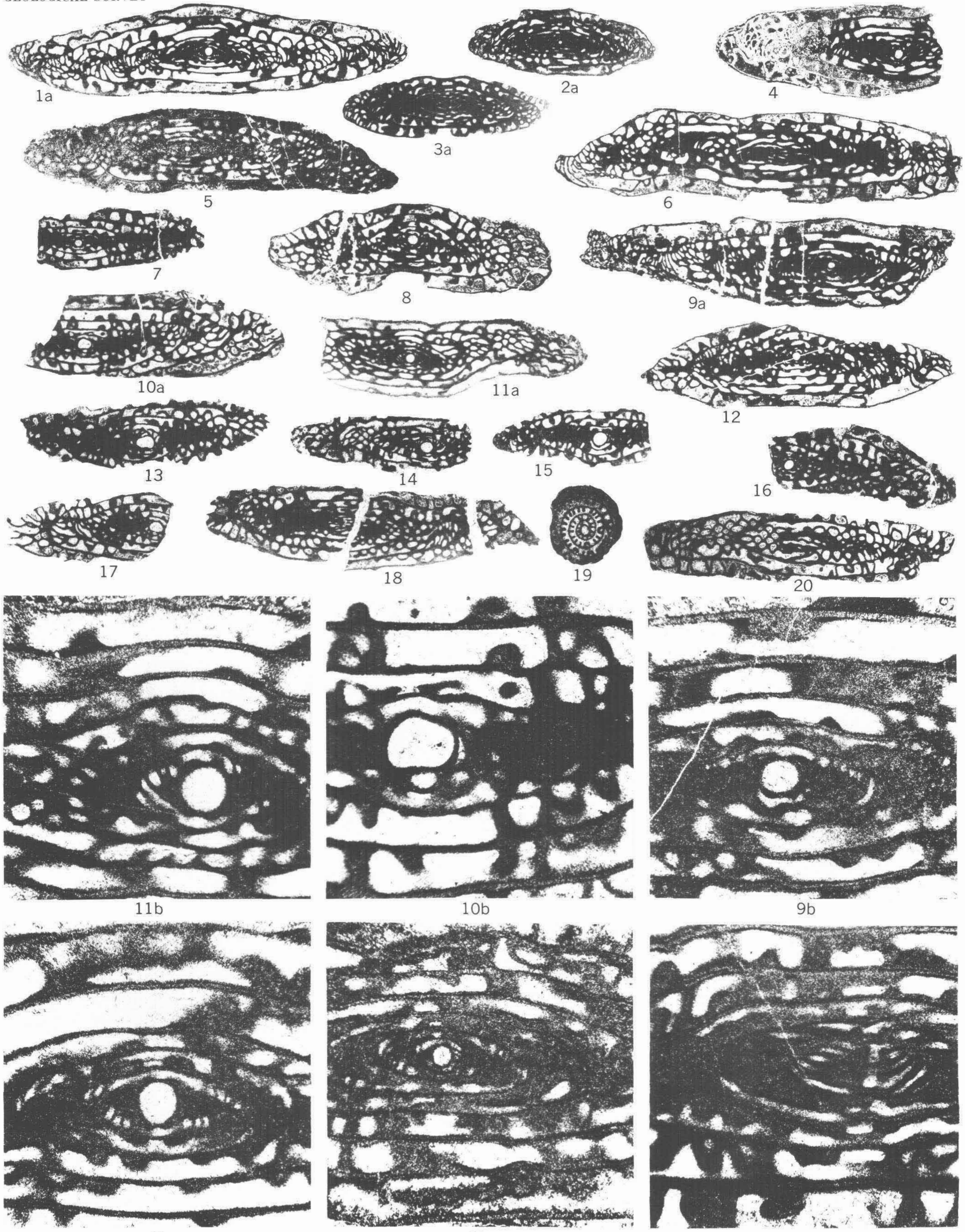

FUSULINA FLEXUOSA DOUGLASS, N. SP., FROM KLAWAK INLET AND PRINCE OF WALES ISLAND